Faculdade de Engenharia da Universidade do Porto

FEUP

Exploring the cardiac response to injury: new clues to enhance repair/regeneration

Sílvia Maria do Couto Rodrigues

Final Version

Dissertation for Integrated Master in Bioengineering - Biomedical Engineering

Supervisor: Diana S Nascimento, PhD
Co-supervisor: Vasco Sampaio-Pinto, MSc

October 2015

Exploring the cardiac response to injury: new clues to enhance repair/regeneration

Dissertation for Integrated Master in Bioengineering - Biomedical Engineering

Workplace:

INEB - Instituto de Engenharia Biomédica

Supervision:

Diana S. Nascimento, PhD [1,2]
Vasco Sampaio-Pinto, MSc [1,2]

Afilliation:

[1] Instituto de Investigação e Inovação em Saúde, Porto, Portugal.
[2] INEB – Instituto Nacional de Engenharia Biomédica

Time Period:

18 Feb 2015 - 31 Oct 2015

Abstract

Since cardiovascular diseases are the leading cause of death worldwide and the mammalian adult heart is incapable of consistent regeneration, countless studies have been performed to characterize the heart injury-response in order to develop new therapeutic alternatives to improve cardiac repair.

In 2011, a proof-of-principle study by Porrello *et al.,* demonstrated that in a restricted time-window after birth murine hearts were able to fully regenerate after apex resection without scar formation. However, when the same injury procedure was performed after post-natal day 7, it results in a reparative response characterized by formation of a fibrotic scar. This work, which constituted a breakthrough in the field, was recently refuted by Anderson *et al.*, whom reported no signs of cardiac regeneration in the first week of post-natal life, setting controversy on the cardiovascular field.

Our work aims to clarify the type of response triggered following neonatal apex resection by detailed analysis of histological/cellular/extracellular matrix (ECM) changes activated after injury. Additionally, a deeper assessment of the neomyogenic potential after injury was performed.

Fine histological analysis of resected hearts show that, despite the proportion of affected tissue is significantly diminished throughout time, only partial recovery is observed 60 days post-resection (dpr) as interstitial scar-tissue is formed in the myocardium. However, systolic heart function was fully restored at 21dpr and no signs of cardiomyocyte (CM) hypertrophy nor compromised vascularization were detected 60 dpr. Furthermore, the neonatal heart response to injury involves the recruitment of inflammatory cells, activation of fibroblasts, and ECM remodeling, namely fibronectin and tenascin-C.

Hereby, we propose a model of neonatal cardiac injury-response that encompasses microenvironmental alterations as main drivers of both reparative and regenerative mechanisms, culminating in the formation of newly formed myocardial tissue with interstitial fibrosis and undetectable impact on systolic function.

Resumo

As doenças cardiovasculares são a principal causa de morte à escala mundial em parte devido ao facto do coração de mamíferos na vida adulta ser desprovido de capacidade regenerativa. Nesse sentido, numerosos estudos têm caracterizado a resposta à lesão em busca de sinais moleculares para integrar novos tratamentos para restaurar a função do miocárdio danificado.

Em 2011, um estudo de prova de princípio demonstrou que, na primeira semana de vida, os corações de murganho são capazes de regenerar na totalidade, sem formação de tecido cicatricial, após remoção do ápice. No entanto, depois do sétimo dia de vida, os corações respondem à lesão de forma diferente e desenvolvem fibrose, produzindo um efeito deletério na função sistólica. Todavia, em 2014, este modelo foi refutado por Andersen *et al.*, o qual reportou que, após a sua replicação, não se observou qualquer recuperação do miocárdio durante a primeira semana de vida pós-natal. Esta publicação estabeleceu controvérsia em torno da existência de regeneração cardíaca em mamíferos e até hoje não existe um consenso entre a comunidade cardiovascular. Posto isto, esta dissertação visa caraterizar mais aprofundadamente a resposta de murganhos neonatais à resseção do ápice cardíaco estudando a dinâmica celular e extracelular ativada após lesão.

Os nossos resultados mostram que os corações não recuperam totalmente até 60 dias após lesão, ainda que ao longo do tempo a lesão (área afetada pela fibrose) vá ficando menos representativa e se verifique restabelecimento da função (21 dias) e neovascularização (60 dias), sem evidência de hipertrofia de cardiomiócitos.

Sumariamente, a resposta neonatal à lesão envolve o recrutamento de células inflamatórias, ativação de fibroblastos, produção e reorganização de matriz extracelular e restabelecimento da vascularização. Os nossos dados apontam ainda para que haja uma recuperação do tecido removido via proliferação de cardiomiócitos residentes.

Em suma os nossos resultados mostram que o coração de murganho ativa eficazmente mecanismos regenerativos que são responsáveis pela recuperação parcial do coração. Contudo estes revelam-se insuficientes e, através de mecanismos reparativos, uma cicatriz fibrótica é gerada.

Acknowledgments

First of all, I would like to thank Professor Perpétua for introducing me and opening new horizons in the world of stem cell biology and, above all, for giving me the opportunity to work in her team.

I also would like to thank Diana for the opportunity to learn under her supervision, for the constant support and availability to talk and guiding me since the monography topic until my final thesis. To Vasco, for letting me continue his investigation topic and teaching me almost everything in lab. Also, for all the advices, willingness to review and discuss questions related to the work and his friendship.

I would like to acknowledge all the members of Stem-Cell Microenvironments in Repair/Regeneration Team. Tatiana for her kindness and help in ImageStream; Tiago for all the beautiful images that he took in the confocal microscope and for making me feel comfortable and confident with my bioengineering background and Rui for all the morning funny conversations and friendship from the very beginning. Finally, I would like to thank Ana Freire, Ana Silva and Francisca for their joy, optimism and help in lab.

Quero agradecer aos meus pais e à minha irmã Inês por todo o apoio que me dão, me facilitarem este percurso e por me incentivarem sempre a fazer mais e melhor. Por fim, e não menos importante, ao João por todo o carinho, paciência, dedicação e disponibilidade para reler este trabalho.

x

Table of Contents

List of Figures

List of tables

Abbreviations and Symbols

Abbreviation List

AMI	Acute Myocardial Infarction
cDNA	Complementary DNA
CM	Cardiomyocyte
CPCs	Cardiac Progenitor Cells
Cx43	Connexin 43
DDR2	Discoidin Receptor Domain 2
Dpr	Days Post Apex Resection
E	Embryonic Day
ECM	Extracellular Matrix
EF	Ejection Fraction
FBS	Fetal Bovine Serum
FGF1	Fibroblast Growth Factor 1
Fn	Fibronectin
FS	Fraction Shortening
HBSS	Hank's Balanced Salt Solution
Hccs	Holocytochrome c synthase
IVS	Interventricular septum
LAD	Left Anterior Descendent
LV	Left Ventricle
MMP	Metalloproteinase
MT	Masson's Trichrome
P	Postnatal Day
PBS	Phosphate-Buffered Saline
PDGFRα	Platelet derived growth factor receptor α
PFA	Paraformaldehyde
PSLAX	Parasternal Long-Axis
ROS	Reactive Oxygen Species
RT-PCR	Real-Time Polimerase Chain Reaction
SAX	Short Axis
Sca1	Stem Cell Antigen 1

s-α-Actinin	sarcomeric-α-Actinin
Tcf21	Transcription Factor 21
TGF-ß	Transforming Growth Factor ß
TIMP	Tissue Inhibitor Metalloproteinase
Tn-C	Tenascin-C
VCAM1	Vascular cell adhesion molecule 1
αSMA	α smooth muscle actinin
µm	micrometer

Chapter 1

Introduction

Cardiovascular diseases are the leading cause of death and disability in the modern World, counting with nearly 17 million deaths according to annual estimates, which corresponds to 30% of global mortality. Indeed, among non-transmissible diseases, cardiovascular diseases are the most lethal, a tendency that has been observed for decades and is predicted to continue [1-3]. Considering the severe socio-economic impact of these estimates, the development of new preventive strategies and therapies is a public health priority [4]. Ischemic heart disease (also known as coronary heart disease), responsible for over 43% of cardiovascular-related deaths, is characterized by the deposition of atherosclerotic plaques in coronary arteries that progressively obstruct their lumen, thereby decreasing blood supply to the heart. This event commonly leads to acute myocardial infarction (AMI) as the result of diminished oxygenation of heart muscle, inducing massive cell death and inflammation [5]. Afterwards, as adult cardiomyocytes (CM) (the contractile unit of the heart) do not proliferate in a sustainable manner, the heart engages on a reparative response towards the damaged tissue replacement by a non-functional fibrotic scar. The combination of muscle loss with the development of myocardial fibrosis, which hampers cardiomyocytic contraction and induces CM hypertrophy, ultimately leads to heart failure [6, 7]. Looking forward to develop efficient therapies for heart failure, cardiovascular research has been fostering studies on the identification of regenerative cues through dissection of evolutionarily conserved heart-injury mechanisms and of heart development.

1.1 - Cardiac Regeneration In Mammals: Opening New Avenues For Therapeutic Alternatives

Regeneration is defined as the complete restoration of lost/damaged tissue both at the histological and functional level. Regeneration is commonly accomplished by cellular proliferation, recapitulating, to a limited extent, the embryonic program that gave rise to the original tissue [8]. In opposition, repair consists in the robust activation of fibrogenic mechanisms to provide tissue structural support by increased production of collagen, which in turn, leads to the formation of a fibrotic scar. Tissue repair is insufficient for effective and permanent re-establishment of tissue histo-functional integrity. The mammalian healing response fluctuates between these two types of response, depending on the tissue-specific stem-cell pool and in the extent of injury. In the case of the adult heart, in contrast with other systems (e.g. intestine, hematopoietic system, skin), the injury response involves mainly reparative mechanisms.

Until the past century the heart was considered a non-regenerative organ, as CMs were thought to enter, shortly after birth, in a non-reversible post-mitotic state with no proliferative capacity [9]. However in the early 2000s, this paradigm changed with reports of progenitor-like cells resident in the adult heart and low-rate CM renewal throughout life (detailed on section 1.2). The first signs of CM proliferation came from AMI injured hearts, in which the border and remote zone exhibits 70 and 24 times more proliferation, respectively, comparing to normal hearts [10]. Bergman *et al*. also reported CM turnover at a rate of approximately 1% at the age of 25, diminishing to approximately 0.45% at the age of 75. Accordingly, even though 50% of CMs are replaced during the normal lifespan, this renewal is clearly insufficient to re-establish the myocardium following cardiac injury, in which nearly 25% of CMs are lost [11-14].

On the other hand, several resident populations of cardiac progenitor cells (CPCs) have been identified in the adult heart. CPCs have been identified by the expression of specific surface markers like c-kit [15], stem cell antigen 1 (Sca1) [16], Isl1 [17] and platelet derived growth factor receptor α (PDGFRα) [18], as well as by multiple physiologic properties and colony formation ability [19]. Moreover, efforts have been made to unequivocally identify and validate adult cardiac stem/progenitor populations, and above all, to clarify their ability to generate CMs [12, 20]. Activation of CPCs was reported *in situ*, through different approaches based on microRNA regulators [21, 22], administration of growth factors [23] and pharmacological agents [24]. Importantly, these cells have been isolated and expanded *in vitro* and subsequently injected in the AMI patients, leading to the reduction of the infarction size; however, long-term effect of cell delivery in a large trial is yet to be performed [25] although phase I clinical trials had been successfully concluded [26]. Overall the present perspective on the field is that CPCs have limited capacity to generate new CMs and their protective effect is mainly mediated by paracrine mechanisms that improve angiogenesis and

cell survival upon AMI [27]. Therefore, despite of being activated upon injury, it is consensual that CPC potential is limited and that their turnover is not sufficient to restore the damaged myocardium [20, 28].

The prospect of endogenous regenerative potential of the adult heart, either by the activation of a progenitor-cell pool or by cell-cycle re-enter of pre-existent CMs, opens new avenues for therapeutic exploitation. Although the reported potential is extensively limited, the question that remains is whether it could be activated by correct environmental signals. Hereupon, cardiovascular field has attracted specialists in stem cell/developmental biology, biomaterials and tissue engineering, whom primary objective is the development of strategies to improve myocardial restoration following injury. In fact, activation of endogenous CPCs, reprogramming of cardiac fibroblasts in CMs and recruitment of non-resident stem cells, in combination with advanced tissue engineering approaches to develop cardiac functional/regenerative patches, are amongst most frequent reported applications [19, 29].

Notwithstanding the reported endogenous regenerative potential of the adult mammalian heart, these mechanisms are clearly insufficient and, in pathological situations, reparative mechanisms are preponderant. Hence, in the quest for novel therapeutic alternatives, cardiovascular research has been fostering the study of heart throughout ontogeny, aiming at unveiling mechanisms of heart morphogenesis which can be further employed in the improvement of adult heart repair. In addition, as other organ-systems display enhanced capacity to regenerate at early ontogenic stages [30], as is the case of the skin, the same was postulated for the heart. Indeed, the first reference to a developmental window for heart regeneration in mammals was provided by Timothy C. Cox and colleagues in 2008. In this study, using a conditional knockout for an enzyme essential in the energetic metabolism of CMs, the authors reported that heterozygous embryos were able to recover from 50% of Hccs (holocytochrome c synthase) deficient cardiac cells at midgestation to 10% at birth. Compensatory increase in the proliferation of healthy cells was shown to mediate the regenerative response that gave rise to a fully functional heart at birth [31]. In 2011, Porrello and colleagues showed, using the murine model, the existence of a time-window in which mammalian cardiac regeneration could occur. In fact, 1-day-old (P1) mice were able to histo-functionally restore the heart following apex resection whereas at P7, this capacity is already lost and extensive fibrosis is observed [32]. Enthusiastically, these findings were corroborated by others, even when different injury models such as AMI, through left anterior descending coronary artery (LAD) ligation [33-35], and cryoinjury [36] were applied. Indeed, in all reported injury-models the restoration of the damaged myocardium is achieved by formation of a blood clot that covered and sealed the injury site, development of an inflammatory response and activation of neovascularisation and neomyogenesis [38]. These

experiments showed that the *de novo* tissue formation is not dependent on CPCs as new CMs arise from pre-existent ones that undergo dedifferentiation and cell-cycle re-entry [35]. Although neonatal cardiac injury models currently available do not reproduce entirely the adult heart physiopathology, the establishment of these models propelled new insight about regenerative mechanisms underlying cardiac injury. Indeed, these models have become a solid platform for the study of mechanisms that contribute to the loss of cardiac regenerative ability from P7 onwards (detailed on section 1.2).

However, in 2014, neonatal heart regeneration has been refuted by Anderson et al, whom reported no signs of cardiac regeneration in the first week of post-natal life, creating controversy in the field [39, 40]. In opposition to the pioneer work, these authors documented a strong inflammatory response in the injury site, followed by massive collagen deposition. Additionally, resected hearts were shown to be smaller than the respective surgical controls, displaying impaired neovascularization and cardiomyocyte proliferation. Importantly, the authors reported similar results in C57BL/6 and in ICR/CD1 mice strains, indicative that murine cardiac response to apex resection is not strain-specific. The authors explained the discrepancies between laboratories to the less detailed histological analysis of the initial paper which could originate underrepresentation of fibrotic lesions. This deceptive outcome has created uncertainties concerning the reproducibility of the neonatal injury model and on the ability of neonates to indeed regenerate their hearts. Nevertheless, it was recently reported that there is a close relationship between the extension of the injury and the outcome of the healing response, which may explain the different results across laboratories [38, 41]. An independent letter led by Kotlikoff remarked that, despite some evident parallelism between Andersen *et al*. findings and their report on neonatal cryoinjury (i.e. CD45$^+$ cell influx, fibrosis and neovascularization of the ablated myocardium) [34], a critical point is missing in Andersen's paper, namely that neomyogenesis is a central feature in neonatal heart repair [42]. Andersen and colleagues counter-argument has been that in their experimental setting, neonatal hearts healed from apex resections with profound scarring and minimal neomyogenesis, therefore lacking substantial regenerative capacity [40].

1.2 - An Integrative Perspective On The Bounderies Of Heart Regeneration In Mammals

The aforementioned studies, together with evidences from other organ-systems [43], are indicative that the capacity to regenerate is dimmed throughout ontogeny. Hence, although the fetus is endowed with cell-plasticity and capability of functional reestablishment following injury, this capacity is lost throughout the postnatal period (the case of the heart) and/or with aging. The study of the heart injury-response throughout

development and post-birth may unveil the mechanisms restricting cardiac regenerative capacity during adulthood, which is of high relevance, considering that their silencing may improve heart repair (detailed in section 1.2.1).

Interestingly, when cardiac regenerative capacity is analysed throughout the evolutionary axis, the mammalian specification is inversely correlated with heart regenerative capacity [44]. Unlike mammals, adult amphibians and fish (namely zebrafish) are capable of cardiac regeneration [45, 46], In line with this, several studies have dissected the mechanisms underlying the cardiac regenerative response of lower vertebrate, aiming at identifying signals/mechanisms of translational relevance [47]. In fact, the identification of mammals and low vertebrates dissimilarities may elucidate the physiological basis for the limited capacity of the mammalian heart (in detail in section 1.2.2)

1.2.1.   *Cardiac regenerative capacity throughout ontogeny*

After parturition, mammalian hearts undergo dramatic alterations that dictate the transition from hyperplasic to hypertrophic growth [48] (Figure 1). Yet, the stimuli that induce CM phenotypic transition are not well understood. Neonatal CMs tend to be smaller in size, contain fewer myofibrils and be mononucleated when compared to adult ones, which may ease their cell-cycle re-rentry [29]. Similarly, during embryogenesis, mammalian hearts develop at expenses of a highly proliferative population of mononucleated CMs that present little organized sarcomeres [49, 50]. Post-birth, most CMs undergo DNA duplication without cytokinesis. Hence, in rodents, CMs undergo mitosis without cytokinesis and CMs become binucleated cells (around 80-90%) with diploid nucleus [14, 51]. In turn, humans CMs undergo mitosis without nuclear division and, therefore, the majority is mononucleated and own a polyploid nucleus [52].

Additionally, mammals face a dramatic environmental shift in the transition between *in utero* and *ex utero* living. Adult zebrafish and fetal mammalian hearts are subjected to low oxygen levels whereas neonatal and adult mammals face an oxygen-rich environment. This has a severe impact over the metabolic status of CMs once while adult zebrafish and fetal mammalian CMs display anaerobic glucose-based metabolism and high proliferative capacity [53, 54], post-natal CMs generate their energy mainly through aerobic oxidative metabolism and the large majority have withdrawn from the cell-cycle [53, 55, 56]. Although mitochondrial oxidative phosphorylation is a more advantageous metabolic pathway, it implies the increase of reactive oxygen species (ROS). Recently, the increase of ROS during the first week of life and consequent activation of DNA damage response pathways has been proposed as a trigger for CM cell-cycle arrest [53].

Interestingly, CM phenotypic shift is accompanied by down-regulation of cell cycle factors and up-regulation of cell cycle inhibitors [57]. The mammalian cell cycle is tightly regulated by cell cycle machinery, combining positive and negative regulators [58]. In line with this, adult-heart growth is essentially achieved by CM hypertrophy rather than CM hyperplasia [59]. In adult mammalian CM, cyclin-dependent kinase/cyclin complex, Myc, E2F transcription factors, cell cycle activators, were demonstrated to be repressed whereas p21, p27, retinoblastoma protein, and cyclin-dependent kinase inhibitors, negative cell cycle regulators, are overexpressed [60-62]. Pasumarthi et al. demonstrated that cyclin D2 expression induces permanent DNA synthesis, reducing fibrosis after AMI [60]. Hence, manipulation of CM cycle activity is a promising strategy to enhance myocardium repopulation following injury. Furthermore, dynamic alterations in DNA methylation were shown to modulate CM phenotype. Upon birth, developmental signalling pathways as well as cell cycle regulator genes are silenced through hypermethylation [63-65].

Recapitulation of developmental signalling pathways in differentiated CMs appears to be another promising strategy to induce CM proliferation. Neuregulin and its receptors, ErbB2 and ErbB4, are involved in cardiac development by promoting CM proliferation and differentiation [66]. In fact, neuregulin and oncostatin administration, an extracellular factor responsible for the activation of neuregulin receptors, were reported to stimulate CM proliferation in physiologic and pathologic scenarios [67-69]. In line with this, other developmental signalling pathways involved in CM cell cycle re-entry (e.g. Hippo and Wnt) have also been targeted [70-73]. Moreover, inhibition of p38α MAPK (negative regulator of CM proliferation in mammals), together with fibroblast growth factor 1 (FGF1) (capable of inducing CMs dedifferentiation) [74, 75], was reported to induce CM proliferation following AMI while contributing to fibrosis and infarct size reduction and increased angiogenesis [76]. Curiously, these mitogenic factors seem to stimulate exclusively mononucleated CMs [69].

The role of microRNAs has also been under tight scrutiny during the postnatal regenerative time-window. Recently, more than 40 microRNAs have been identified as mitotic triggers for CM although deeper studies are required in order to manipulate them for future therapies [77, 78]. For example, after birth, overexpression of miR-15 family is observed in murine hearts which coincides with the loss of CM proliferative capacity [35]. Interestingly, miR-19 (a member of mir-15 family) overexpression inhibits neonatal heart regeneration [35].

Furthermore, extracellular matrix (ECM) also effectively modulates cell behaviour either via cell-matrix interactions, paracrine factors incorporated within the network and by molecular and mechanistic properties of ECM [79]. Numerous studies have shown that cells are responsive to the microenvironment and, since there is a shift on ECM properties throughout development, this structure may instruct cells in an ontogenetic-dependent manner and impact on the regenerative capacity [80, 81]. In physiological conditions, the

myocardium is gradually enriched in collagen type I, which becomes the most predominant cardiac ECM protein in the adulthood, whereas fibronectin (Fn) and elastin become increasing less represented. These composition changes strongly increase ventricular stiffness, contrasting with the cardiac regenerative potential that follows the opposite trend [82].
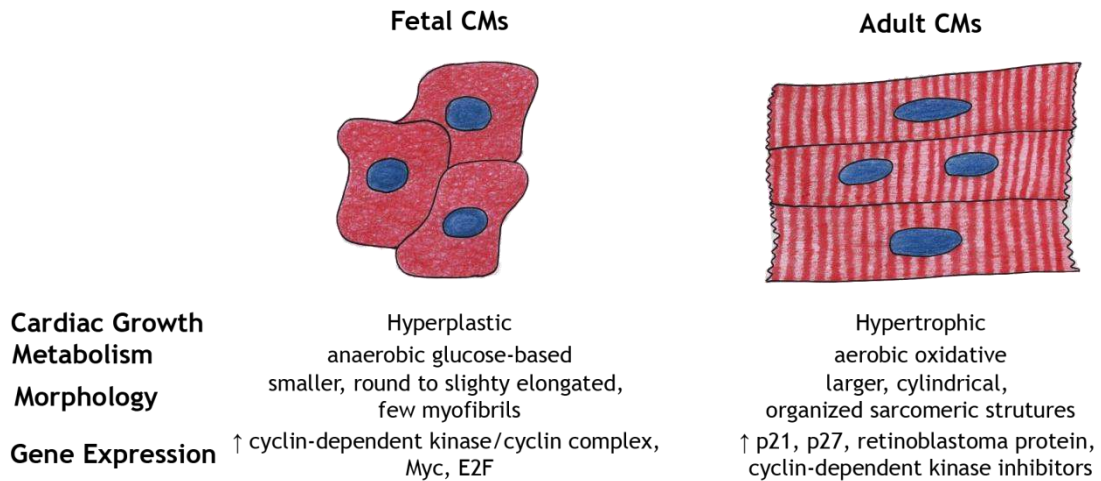

	Fetal CMs	**Adult CMs**
Cardiac Growth	Hyperplastic	Hypertrophic
Metabolism	anaerobic glucose-based	aerobic oxidative
Morphology	smaller, round to slighty elongated, few myofibrils	larger, cylindrical, organized sarcomeric strutures
Gene Expression	↑ cyclin-dependent kinase/cyclin complex, Myc, E2F	↑ p21, p27, retinoblastoma protein, cyclin-dependent kinase inhibitors

Figure 1. Schematic differences between fetal and post-natal CMs. After birth, mammalian hearts undergo dramatic alterations that dictate the transition from hyperplasic to hypertrophic growth, which is accompanied by metabolic, morphologic and gene expression modifications [83].

1.2.2.   Phylogenetic axis of cardiac regeneration

Owing to increased energetic requirements, mammals have developed different mechanisms at the anatomic, histological and biochemical level that are inversely correlated with heart regenerative capacity [44] (Figure 2). In fact, throughout vertebrate evolution a specialized electrical conduction system, where the transmission of electromechanical stimulus is achieved through gap junctions, was developed. More than 20 different connexin family members are found in mammals, allowing rapid and synchronous contractions. In agreement, an altered expression and distribution of connexin-43 (Cx43), a structural protein of gap junctions, is correlated to the development of cardiomyopathies, such as hypertrophy and ischemia [84-87].

Mammals have developed higher blood pressure when compared with adult zebrafish. In an injury scenario, zebrafish are able to quickly seal the wounded area with a blood clot while CMs dedifferentiate, disassemble their sarcomeric structure and detach from one another [88, 89]. In opposition, due to increased blood-pressure levels, the mammalian heart requires a higher structural support to counteract bleeding, thus favouring scarring [83].

The inflammatory response has been also suggested to be a key player in regeneration [90] since it is required for removal of cell debris, recruitment other cell types,

via soluble factor release, and to promote the formation of a transitional matrix that seals the injured area. However, prolonged inflammation limits tissue expansion of the injured area by an excessive ECM deposition that hampers cardiomyocytic survival [90]. Apart from an innate immune system, lower vertebrates present an incomplete adaptive immunity, which largely differs from mice that develops this system around birth or even from humans where the adaptive immunity is already present at gestational week 10 [91, 92]. Several studies have correlated the loss of immune tolerance with a restricted regenerative capacity [93-96]. More recently, postnatal changes in murine immune system corroborated this premise. Different molecular signatures were identified in monocytes and macrophages from regenerative (P1) and reparative (P14) periods following AMI. Indeed, P1 macrophages express pro-angiogenic cytokines, which are crucial for a successful tissue restoration. Interestingly, depletion of macrophages in neonatal regenerative period led to of the loss of the regenerative capacity, implicating the immune response as major player on cardiac regeneration [97, 98].

Considering the extracellular environment, several ECM proteins are required for efficient zebrafish heart regeneration. Indeed, apex-resection promotes the formation of a provisional fibrin/Fn-rich matrix that allows CM migration to the injury site. Fn was shown to be extensively deposited at the injury site by epicardial cells and its relevance became undeniable once its deletion impaired cardiac regeneration [99]. In adult newts hyaluronic acid, Fn and tenascin-C (Tn-C) are also deposited following apex resection, and deposition of Tn-C was shown to be sufficient to induce CM proliferation [100]. Contrasting with fish and amphibians that own a soft ECM throughout life and during injury response, mammals exhibit exacerbated production of collagen type I and III, as well as fibre rearrangement following injury. The increased crosslink between ECM components leads to the escalation of myocardial elastic modulus [81], which limits cellular movement [101] and is on the origin of cardiac dysfunction [102]. Distinct reports have shown that fibroblast distribution is different between lower and higher vertebrates. In mammals, fibroblasts are one of the most represented cell types while, in lower vertebrates, they are less frequent and dispersed in the myocardium [103]. Not surprisingly, an extensive and well-organized cardiac fibroblast structure in mammals is suggested to have deleterious impact on regeneration [103] once they are not only responsible for scar formation but also for triggering CM cell cycle withdrawal [104].

Importantly, a pattern of biological events is transversal to all vertebrates. Firstly, a blood clot is formed at the injury site that seals the lumen and induces an early and strong inflammatory response. Gradually, the blood clot and fibrotic tissue are replaced by novel CMs arising from pre-existing ones. Fibroblast recruitment, extracellular matrix deposition and epicardial genes activation are other hallmarks of heart regenerative response of low

vertebrates [105] which are yet to be explored in mammals and will partially be addressed in this dissertation (Chapter 2 and 5).
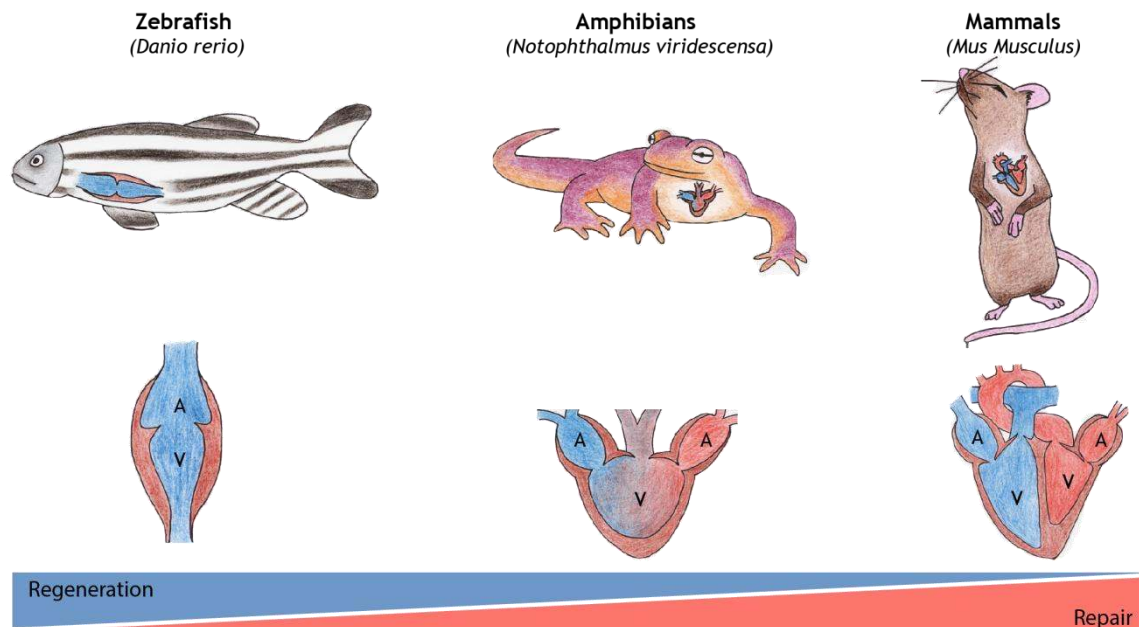
Figure 2. Heart anatomy and regenerative potential throughout the phylogenetic axis. Within vertebrates, the heart exhibits anatomic and physiologic variability owing to adaptation to distinct environments. The multiple mechanisms acquired during evolution are inversely correlated with heart regenerative capacity [44].

1.3 - Role of Fibroblasts in Cardiac Injury Response

Scarring is a major obstacle to the functional recovery of the injured mammalian heart. It is widely recognized that cardiac fibroblasts are critically involved in the reparative response following myocardial infarction and in cardiac ECM remodeling, depositing large amounts of collagen [103]. Even still, the specific contribution of non-myocardial cardiac cells and extracellular matrix (ECM) in neonatal regenerative cardiac response is yet to be determined.

Among cardiac cellular compartment in the adult heart, cardiac fibroblasts are the most predominant ones, accounting for almost two thirds of the myocardial cells [106]. They are the main producers of ECM, synthesizing Fn (most abundant non collagenous protein), vitronectin, collagen types I, III and V among other ECM proteins in different proportions [80, 107]. In homeostatic conditions, fibroblasts provide mechanical support for CMs, modulate heart conduction system and transmit the contractile force [108, 109].

Apart from a structural role, in development, fibroblasts interact with CMs through paracrine factors and cell-cell interactions. Thus, the latter are able to mediate CM

proliferation via Fn/ß1-integrin-mediated pathway and by production of collagen and heparin-binding EGF-like growth factor [104]. Within the first two weeks of life there is a massive increase on cardiac fibroblast population, in a period coincident with the loss of neonatal regenerative capacity [109].

Unsurprisingly, cardiac fibroblasts are mainly recognized by their activation upon MI. Initially, a rapid inflammatory response is triggered by a massive cell death, where immune cells are recruited by factors released by the necrotic/apoptotic cells and by inflammatory cells [110]. Inflammation resolution induces differentiation of fibroblasts into myofibroblasts [111, 112]. Finally, myofibroblasts and resident fibroblasts deposit large amounts of ECM proteins mainly collagen type I and III, emerging a non-functional fibrotic scar [113]. Additionally, fibroblasts are able to modulate angiogenesis, instruct neighbouring CMs and regulate matrix remodelling through expression of proteolytic enzymes (e.g matrix metalloproteinases (MMPs)) and their inhibitors (e.g tissue inhibitor metalloproteinases (TIMPs)) [104, 109]. In this sense, modulation of fibroblast activity can impact the balance between regeneration versus reparative healing after cardiac injury and may constitute an important therapeutic target.

Frustratingly, the knowledge of this population has been hampered by the absence of reliable markers. Some efforts have been made to overcome this issue, namely by using some proteins to prospectively identify fibroblasts. Vimentin and fibroblast specific protein (FSP1) have been widely used in this purpose but lack specificity since they can be expressed by endothelial and smooth muscle cells or by lymphocytes, monocytes and macrophages [111, 114-116]. Additionally, CD90 (Thy 1) [117], transcription factor 21 (tcf-21) [118], discoidin receptor domain 2 (DDR 2) [119], periostin [120] have also been used. However, considering the heterogeneity this population of cells, results obtained from the usage of a single marker should be carefully interpreted. Additionally, the differentiation of fibroblasts into myofibroblasts, a hallmark in reparative response, is mainly detected by the expression of α-smooth-muscle actin (α-SMA).

Chapter 2

Preliminary Data

Cardiovascular community has been focused on investigating mechanisms that govern neonatal regeneration, aiming to extend this ability to later periods in life [32-36, 38]. However, in 2014, the regenerative capacity of neonatal mice has been questioned and, thus, a consensus on the field is yet to be reached [39, 40].

The neonatal apex resection model has been established in our laboratory (Figure 3) using the same protocol described originally by Porrello *et al.* [32]. However, we performed the procedure on inbred C57BL/6 strain at P1.5 contrasting to the outbred ICR/CD-1 P1 mice used by Porrello *et al.*. Immediately after surgery, the survival rate is not significantly different between apex-resected animals (84.2%) and the surgical controls (86.5%). Notwithstanding, this value is considerably affected by maternal cannibalism in the first 48h post-surgery, lowering to approximately 48% and 67% for apex-resection and sham groups, respectively (Figure 4).
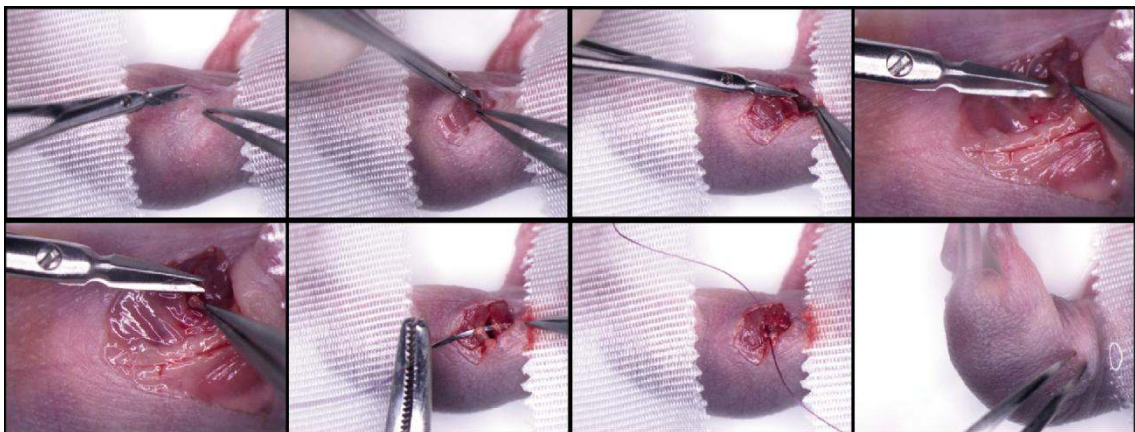
Figure 3. Neonatal heart apex-resection injury model. The heart was assessed by opening the thorax in the 4th intercostal space and the apex was cut.
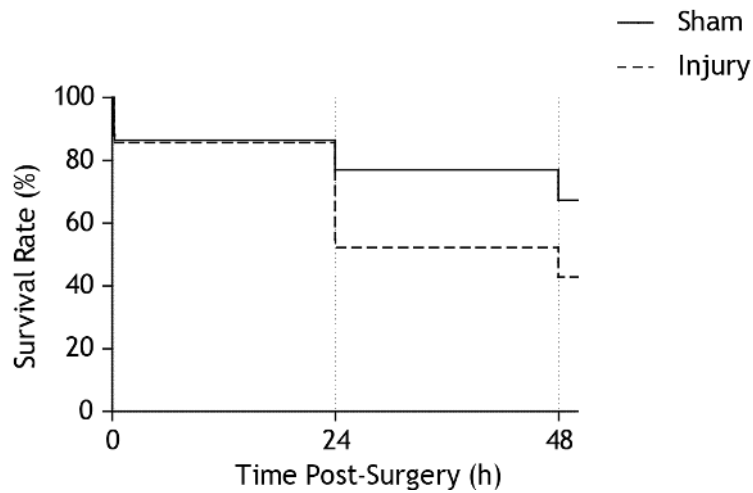
Figure 4. Survival rate post-surgery. The survival rate to surgery in both group set on approximately 85%. This value was considerably affected by maternal cannibalism during the first 48h post-surgery. Sham (n=52); Injury (n=38).

Twenty-one days after apex resection (dpr), animals do not show alterations on cardiac systolic function, as no differences were observed in ejection fraction and fraction shortening between resected and sham-operated animals (Figure 5). Although no differences were observed at the functional level, a small amount of myocardial fibrosis is noticeable at the resected area (Figure 6).
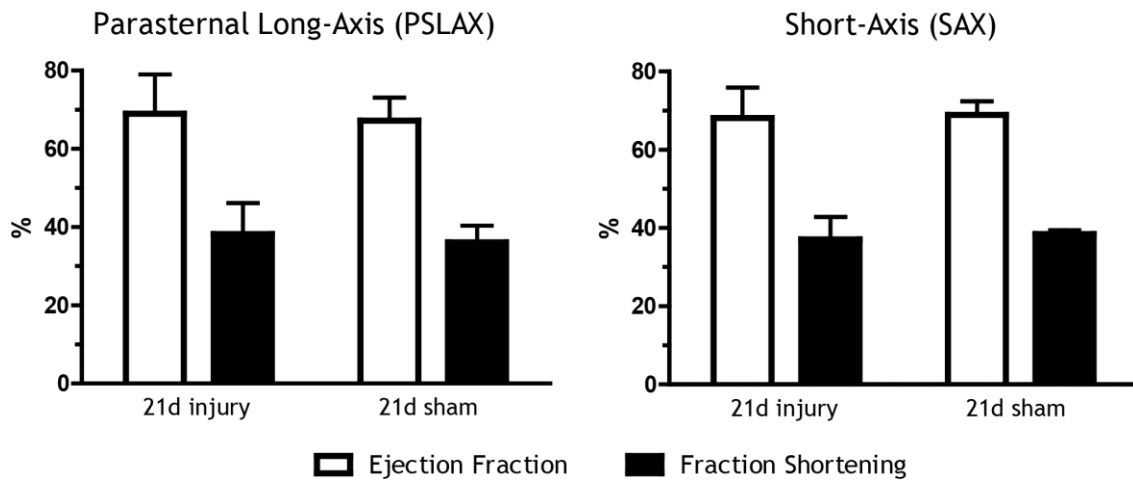
Figure 5. Functional characterization of the neonatal cardiac injury model. No alterations in ejection fraction or fraction shortening were observed between groups in PSLAX and SAX views. Values are presented as means+ standard deviation (SD). 21d Sham (n=3), 21d Injury (n=4).
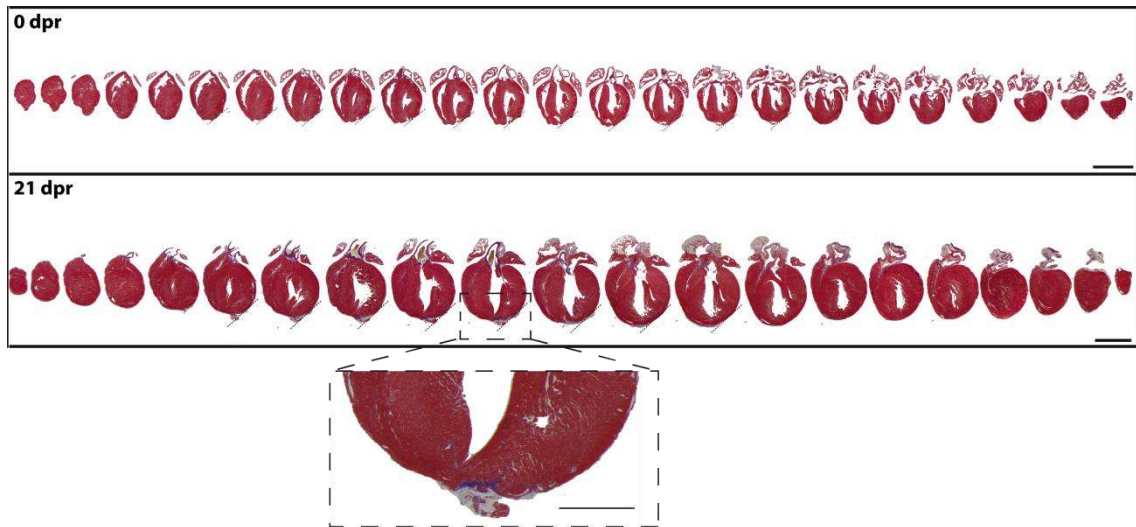
Figure 6. Histological characterization of the neonatal cardiac injury model. Masson's Trichrome representative sections of apex-resected hearts at 0 and 21 dpr. Scale bar: 2mm. Higher power image (below) empathizes collagen deposition in apex region. Scale bar:1mm.

Additionally, extracellular and cellular dynamics following apex resection were assessed (Figure 7). Immediately after injury, disruption on the expression pattern of sarcomeric-α-actinin (s-α-actinin) and laminin is observed although partial recovery of the myocardium was detected at 21 dpr. Furthermore, the recruitment of inflammatory cells, ECM production and fibroblast activation are also involved in injury response. Hematopoietic cells (CD45 expressing cells) are present from 0 dpr and its frequency increases until 5dpr while, from this time-point onwards, a dramatic decrease of CD45-expressing cells is observed which may relate with the resolution of inflammation. Deposition of Fn and Tn-C, in the outer surface of the apex-resected area, is already evident at 48 hpr and remains elevated until 14 dpr for Fn and until 21 dpr for Tn-C. Differently, α-SMA and vimentin expressing cell rates steadily increase until 7 dpr, most likely representing the proliferation and differentiation of cardiac fibroblasts into myofibroblasts. The sham-operated animals were also evaluated for these processes; however, they maintained the myocardium structure throughout time with no significant signs of inflammation or fibrosis.
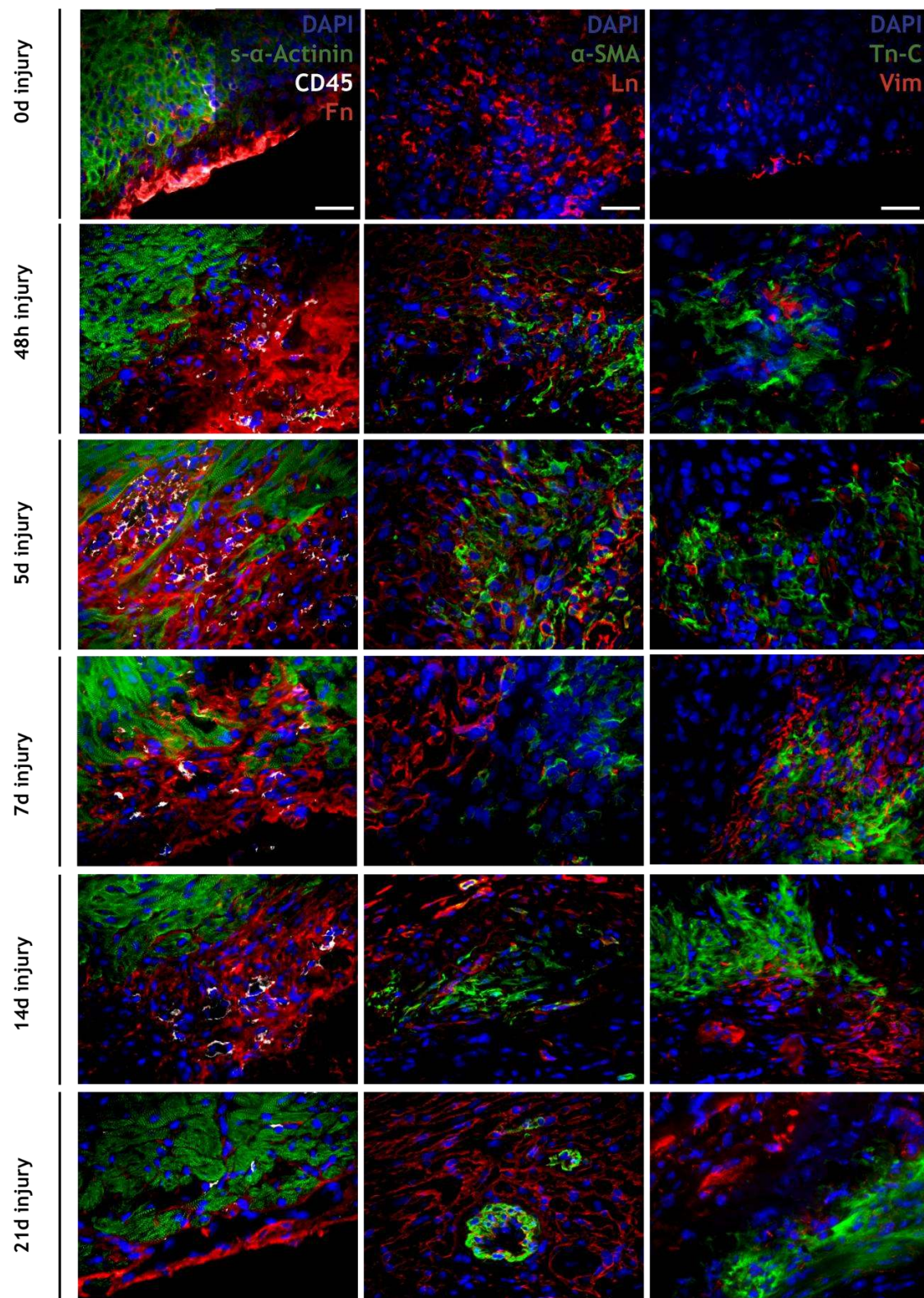
Figure 7. Representative images of cardiac cells co-localization with ECM components in the injury site at 0, 2, 5, 7, 14 and 21 days post-apex resection. The disruption of the myocardium caused by the apex resection is shown by a disorganized pattern of s-α-actinin and laminin until 14 days post apex resection. From 48 hours up to 21 days following apex resection the cellular and extracellular composition of the injured site is dramatically altered, culminating in the partial reestablishment of the removed myocardium at 21dpr. Scale-bars: 30 μm. n=3

Given the activation of fibroblasts upon injury and aiming to dissect their role in regenerative/reparative mechanisms, a preliminary phenotypic characterization was performed throughout ontogeny. Cardiac fibroblasts were defined as CD90 expressing cells after exclusion of CD31 (endothelial marker), CD45 (hematopoietic marker) and TER119 (erythrocytes marker) expressing cells. Briefly, the analysis shows an increase in the number of CD90 expressing cells among development, which is in accordance with previous reports [109] (Figure 8 (A)). Moreover, we analyzed the expression of mesenchymal-associated markers and cell adhesion molecules within CD90$^+$ population. Sca1 protein has been related with the identification of heart resident progenitors and Sca1$^+$ cells has been implicated in the regenerative potential following AMI [121]. Notwithstanding, Sca-1 expression has been observed in the resident fibroblast population of several organs (e.g. skin and lungs) [20]. Finally, CD140a (also known as PDGFRα) is required for epicardial-specification through epithelial-to-mesenchymal transition in order to originate cardiac fibroblasts during development [122] and this marker has been reported to identify cardiac fibroblast subsets in the adulthood. We observed that CD90$^+$CD140a$^+$ and CD90$^+$Sca-1$^+$ fibroblast significantly increase post-birth, which accounts for the fact that fibroblast frequency in the heart is increased with age. As anticipated, we did not observe significant changes on the expression of CD44 throughout ontogeny since this molecule is associated to the differentiation of fibroblasts into myofibroblasts [123] and to fibroblast tissue-invasive capacity [124].

Moreover, cardiac fibroblasts become the preponderant proliferative cells in adulthood, given the increment on Sca1 expressing cells (from residual at P2 to 70% in adulthood) (Figure 8 (B)). Within the proliferative compartment a phenotypic switch between the fetal and adult life could be detected. While at E17, the majority of proliferative cells are Sca-1$^-$ and CD90$^-$, in the adult life the majority of the proliferative compartment expresses these markers.

Overall, our preliminary data is yet inconclusive regarding the activation of regenerative mechanisms and a deeper analysis is required to understand the mechanisms underlying neonatal cardiac injury response.
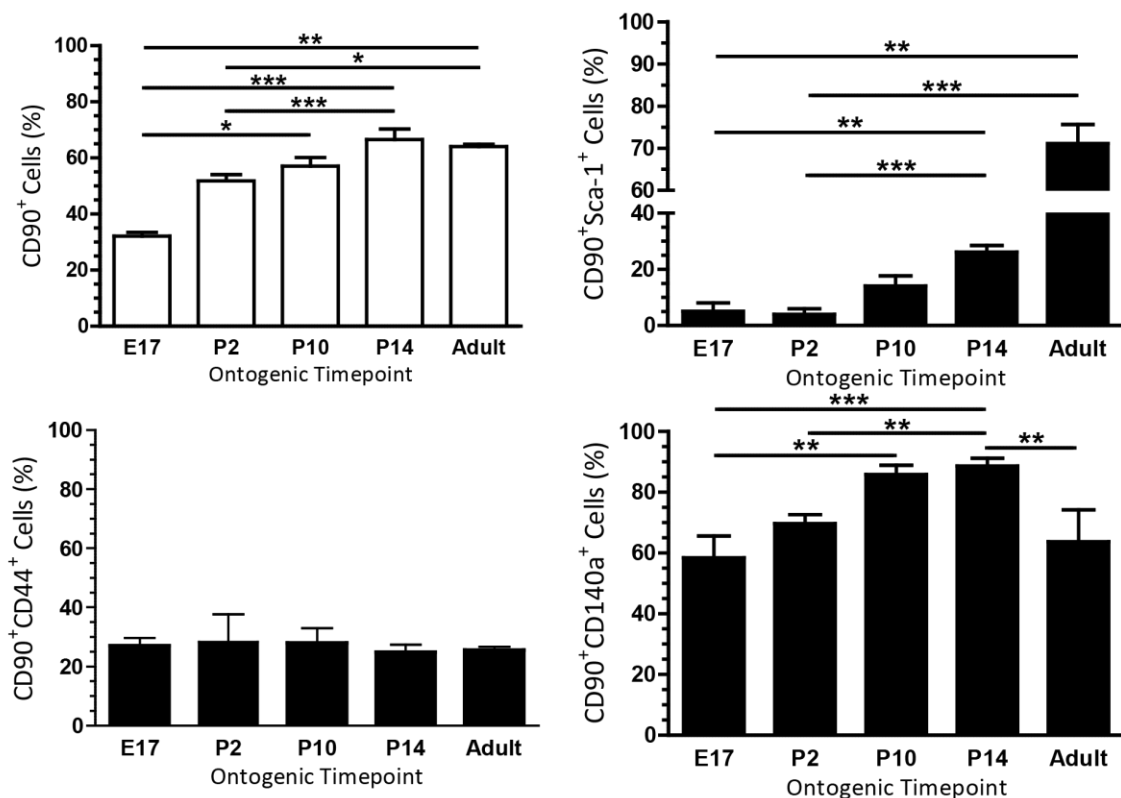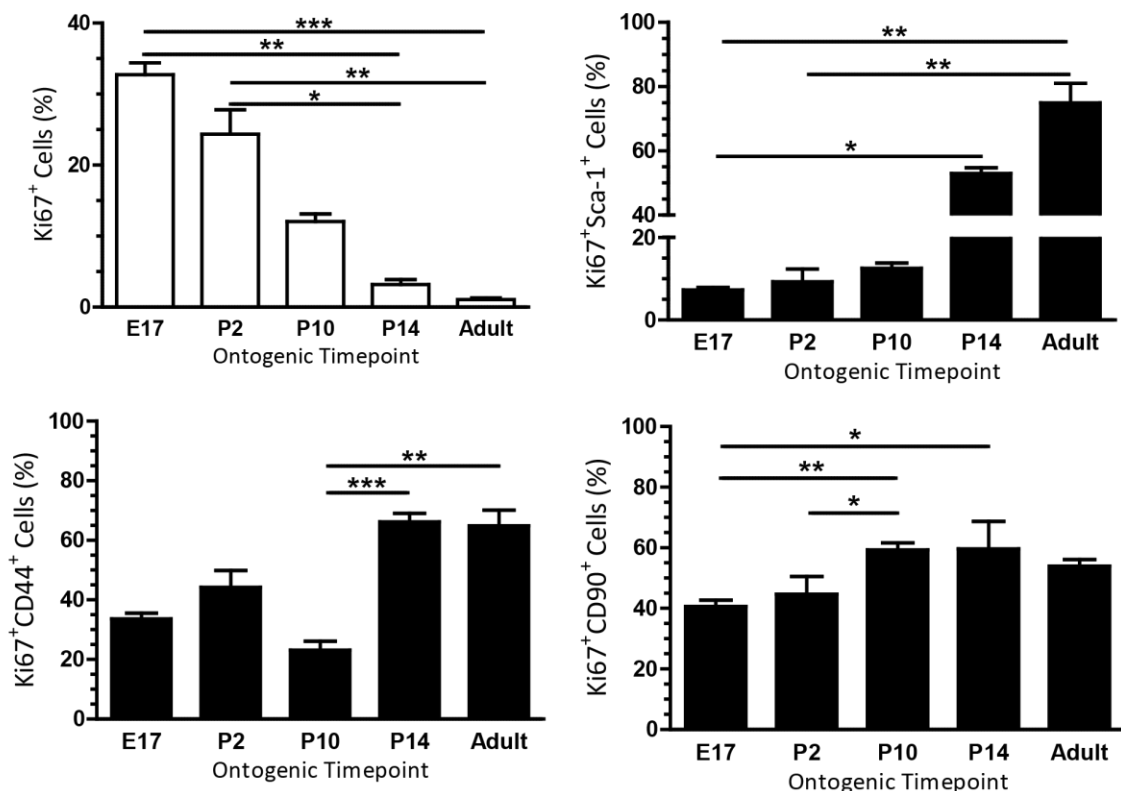
Figure 8. Phenotypic characterization of cardiac fibroblasts throughout ontogeny. (A) Within the stromal compartment i.e. CD45-CD31-TER119-, cardiac fibroblasts were identified by the expression of CD90 and the expression of mesenchymal-affiliated markers and adhesion molecules was further investigated. **(B)** Phenotypic characterization of proliferative stromal compartment throughout ontogeny. The proliferative stromal compartment was ascribed by Ki67 expression profile and it was further characterized E17 (n=6); P2 (n=11); P10 (n=11); P14 (n=11); Adult (n=4).

Chapter 3

Aims

Taking into account the controversy on the cardiovascular field and the preliminary work described above, the broader aims of the herein MSc dissertation are: (i) **to clarify the type of response triggered following neonatal apex resection** and to (ii) **conclude whether this injury-model constitute a valid tool to study molecular mechanisms underlying cardiac regeneration.**

To attain this major goals we will:

- ✓ Follow-up the injury response for longer periods (60 days post-surgery);
- ✓ Assess CM proliferation and CM hypertrophy by morphometric analysis;
- ✓ Dissect ECM production and ECM-producing cells types during neonatal injury response;
- ✓ Evaluate the activation of different cardiac fibroblast subsets upon injury.

Chapter 4

Materials and Methods

4.1 - Animals

All animal-testing procedures were subjected to approval by the IBMC-INEB (Instituto de Biologia Molecular e Celular– Instituto de Engenharia Biomédica) Animal Ethics Committee, and to the Direcção Geral de Veterinária (permit 022793), and are in conformity with the Directive 2010/63/EU of the European Parliament. Humane end-points were followed in accordance to the OECD Guidance Document on the Recognition, Assessment, and Use of Clinical Signs as Humane End points for Experimental Animals Used in Safety Evaluation.

4.2 - Neonatal Murine Apex Resection Injury Model

The neonatal injury model consists in the apex surgical resection of post-natal day (P)1-1.5 C57BL/6 mice. The executed protocol was based in Porrello *et al*. experiments [32]. Animals were anesthetized by hypothermia during precisely three minutes to cease respiratory movements and heart contractions and lose the paw withdrawal reflex. Animals were immobilized with sealing tape in a lateral position, exposing the left-side flank. Then, the skin was cut and muscles disrupted until ribs were observed. The thoracic cavity was opened in the 4th intercostal space and the left ventricle apex cut with fine scissors. The thorax and skin were closed by 7-0 absorbable suture (Coated Vicryl Ethicon) and animals were recovered from anaesthesia under an infrared lamp together with stimulation by tightening the paw until regular breathing was observed. Once neonates are dependent on the mother for temperature regulation and nutrition, the operated animals were replaced on the progenitor cage. During all the procedure, except throughout surgery, neonates were

warmed by warming pads and infrared light. The surgical controls (sham-operated mice) underwent the same procedure in exception to cardiac manipulation.

4.3 -   Heart Fixation and Processing

Hearts were harvested at 0, 7 and 60 days post-surgery. Prior harvesting, animals were weighted and then hearts were carefully removed from the thoracic cavity, while surrounding tissues were cut with the assistance of a stereomicroscope. To assess injury extension, hearts were photographed and its vertical axis (comprised between the great vessels and apex) was measured using ImageJ software (v 2.0.0).

4.4.1. Gelatin Embedding

Tissue processing for cryosectioning involved 3 consecutive solution submersions where each of them lasted for 24 hours at 4^{0}C. The first solution fixed the tissue and it is composed by: 0.2% paraformaldehyde in 0.12M phosphate buffer; the second of 4% sucrose in 0.12M phosphate buffer, and the last one of 15% sucrose in 0.12M phosphate buffer. In the fourth step, hearts were incubated in 15% sucrose and 7.5% gelatin in 0.12M phosphate buffer during 1 hour at 37ºC. Finally, hearts were transferred into a mold containing the latter warmed solution and placed into a recipient containing dry-ice-chilled 2-methylbutane (GPR Rectapur, VWR). Frozen hearts were stored at -80^{0}C. For immunofluorescence, 7 day post-surgery hearts were completely cut from the anterior to posterior side into 5 μm sections using a refrigerated microtome (Microtom HM 550, Thermo Scientific).

4.4.2. Paraffin Embedding

Before paraffin embedding, hearts were submersed in phosphate-buffered saline (PBS 1x) and fixed in 10% formalin neutral buffer (VWR BDH & Prolabo) during 24 hours at room temperature. Then, hearts were processed during a total time of 12 hours in an automated system through successive PBS washes, crescent series of alcohols (Aga), Clear Rite 3® (Richard-Allan Scientific) and Shandon Histoplast (Thermo Scientific) at 56ºC. Finally, hearts were included in paraffin and sectioned longitudinally in 3 μm sections, using a microtome (RM2255, Leica). For representative sampling of the heart 10 series of cuts equally distanced were obtained. The distance between series was specific according to ontogenic stage: no sampling, 30 μm and 50 μm for 0, 21 and 60 days post-injury/sham hearts, respectively.

4.4 -   Histological Examination

Paraffin heart sections were dewaxed through three successive xylene solution submersions and then rehydrated by passing in a decrease series of ethanol solutions (100%, 96%, 70% and 50%) prior to modified Masson's Trichrome (MT) stains. The MT was performed according to the Trichrome (Masson) Stain kit (HT15-1KT, Sigma-Aldrich) modified in the following steps. Firstly, nuclei were pre-stained with Celestine Blue solution (5 min) after staining with Gill's Hematoxylin (5 min). Then, an incubation for 1 hour in aqueous Bouin solution was performed to promote uniform staining followed by immersion in a Biebrich Scarlet-Fuchsin solution (5 min). To conclude the staining, sections were immersed in a Biebrich Scarlet-Fuchsin solution (5 min), followed by a working Phosphotungstic /Phosphomolybdic acid solution (5 min), which acts as a mordant, and finally in Aniline Blue solution (5 min). Between the immersion in all solutions, samples were rinsed in deionized water with the exception of Gill's Hematoxylin where sections were washed in tap water (2min). Sections were diafanized in xylene and mounted in DPX Mountant for histology (06522, Sigma-Aldrich®) after a previous incubation at 37°C to dry. Whole-heart images were acquired in an Olympus SZX10 stereomicroscope. High-magnification images were acquired in an Olympus CX31 optical microscope and an Olympus DP25-4 camera.

The cross-sectional area of CMs was quantified using AxionVision software (V 4.9 1.0, Zeiss) based on MT staining. Only CMs that were aligned transversely were considered for the quantification of the CM surface area and in each section 30 CMs were randomly chosen per area (apex and remote).

4.5 -   Immunohistochemistry

Paraffin-sections, obtained as previously described, were dewaxed and rehydrated by three changes in xylene, followed by sequential alcohol gradients and rinsing in deionized water. Cryosections did not required these steps.

If antigen retrieval was necessary, heat-induced epitope retrieval (HIER) or enzymatic epitope retrieval (PrER) were applied. For HIER, sections were incubated for 35 minutes at 98°C on a water bath, in 10mM sodium citrate, pH 6.0 or in 10mM Tris 1mM EDTA (Tris-EDTA), pH 9.0 and let to cool down for 20 minutes at room temperature. For PrER, sections were incubated for 10-30 minutes in proteinase-K (0,2mg/mL in tris-EDTA pH8), acid pepsin (750μL 1% pepsin stock + 743uL HCl 1M up to 75 mL dH2O) or pronase (1mg/mL in 1x PBS) at 37°C.

Sections were permeabilized with 0.2% Triton X-100 (for intracytoplasmic motifs) or with 1% Triton X-100 (for nuclear stainings). Tissue sections were blocked for 1 hour in 4% FBS and 1% bovine serum albumine (BSA). If the primary antibody was produced in mouse, M.O.M.ᴛᴍ Immunodetection Kit (Vector Lab) was applied to enable blocking of endogenous Fc receptors that could be recognized by the secondary antibody [125]. Incubation with primary antibody was performed in a humidified chamber 2 hours at room temperature (RT) or, alternatively, overnight at 4°C. Then, sections were incubated with the secondary antibody during 1 hour at RT. In order to amplify the fluorescence intensity of several antibodies, streptavidin conjugated fluorophores were used: Streptavidin conjugated with Alexa 555 (S32355, Invitrogen), at 1:500 dilution, Streptavidin conjugated with Alexa 647 (S21374, Life Technologies), at 1:400 dilution or Streptavidin conjugated with Allophycocyanin (APC) (SA1005, Life Technologies), at 1:100 dilution during 20 min.

Sections were mounted with Fluoroshieldᴛᴍ with DAPI (F6182, Sigma-Aldrich) and were observed either in a Zeiss Axiovert 200M, an inverted fluorescence microscope, in a Leica SP2 AOBS SE or Leica TCS SP5II laser scanning confocal microscope (Leica Microsystems) or in GE IN Cell Analyzer 2000, an High-Content Screening microscope.

Table 1. List of primary antibodies used and working conditions.

Antibody	Dilution	Reference	Antigen Retrieval*
Sarcomeric-α-Actinin (Mouse IgG)	1:400	A7811, Sigma	-
Vimentin (Mouse IgG1/K)	1:50	MS-129-P, Thermo	-
CD31 (Goat IgG)	1:250	sc-1506, Santa Cruz Biotechnology	Tris-EDTA, pH 9.0
CD45 (Goat IgG)	1:100	AF114, R&D	-
Alpha-Smooth Muscle Actin (Mouse IgG)	1:400	A5228, Sigma	-
phosphorylated-histone3 (Rabbit IgG)	1:800	#3377, Cell Signaling	-
Fibronectin (Rabbit IgG)	1:400	F-3648, Sigma	-
Laminin (Rabbit IgG)	1:400	L9393, Sigma-Aldrich	-
Tenascin-C (Rat IgG)	1:100	LAT-2, Sonnbg	-
Collagen I (Mouse IgG)	1:100	C2456, Sigma	Pronase (1mg/mL in 1x PBS) at 37°C for 30'
B-1 Integrin (Rat IgG)	1:50	14-0292, eBiosciences	-
Conexin-43 (Goat IgG)	1:400	AB0015-200, SicGen	Sodium citrate, pH 6.0

*Conditions performed in paraffin sections

Table 2. List of secondary antibodies used and working dilutions.

Antibody	Dilution	Reference
Alexa Fluor 488 Donkey anti Mouse IgG	1:1000	A-21202, Invitrogen
Alexa Fluor 594 Donkey anti Mouse IgG	1:1000	A-21203, Invitrogen
Alexa Fluor 488 Goat anti Mouse IgG	1:1000	A11017, Molecular Probes
Alexa Fluor 488 Donkey anti Rabbit IgG	1:1000	A-11055, Invitrogen
Alexa Fluor 568 Donkey anti Rabbit IgG	1:1000	A-10042, Invitrogen
Alexa Fluor 633 Goat anti Rabbit IgG	1:1000	A21070, Molecular Probes
Biotinylated Donkey anti Rabbit IgG	1:250	A16033, Life Technologies
Alexa Fluor 568 Donkey anti Goat IgG	1:1000	A-11057, Invitrogen
Biotinylated Donkey anti Goat IgG	1:250	A16009, Life Technologies
Alexa Fluor 488 Donkey anti Rat IgG	1:1000	A-21208, Invitrogen
Alexa Fluor 568 Goat anti Rat IgG	1:1000	A11077, Molecular Probes
MOM Biotinylated anti mouse Ig	1:250	MKB-2225, Vector Laboratories
Biotinylated Goat anti Rat IgG	1:200	BA-9400, Vector Laboratories

4.6 - High Content Screening: Cardiomyocytic Proliferation and Neovascularization Assessment

After the acquisition using GE IN Cell Analyzer 2000, the proliferative response of neonatal murine hearts at 7d injury and (neo)vascularization at 60d injury were evaluated using IN Cell Developer Software (v1.9.2). This software segments each acquisition channel and create artificial masks for each structure of interest. CMs were classified proliferative when the software detected an overlap between DAPI and s-α-Actinin masks and an intensity in pH-3 channel above a predefined threshold. Similarly, the total number of endothelial cells was accessed by co localization of DAPI and CD31 expression. The results were normalized per area which was quantified in advance by the assembly of individual pictures in ImageJ software v2.0.0.

4.7 - Flow Cytometry and Cell Sorting

Flow cytometry was performed to ascertain cardiac fibroblast activation at 7d post-surgery. Herein, this population was selected based on the expression of CD90 and lack of expression of CD31, CD45 and TER119. Cardiac cells were isolated by digestion of cardiac tissue fragments with crude collagenase (C2139, Sigma-Aldrich®) at 200µg/ml concentration and DNase (A3778, VWR) at 60U/ml in hanks balanced salt solution (HBSS) (H9269, Sigma-Aldrich®). Collagenase digestions were performed during 15 min at 37ºC until no tissue was observed by visual inspection. After each digestion, the suspension was decanted, the media collected (cellular portion) and a new collagenase/DNase solution was added to the

remaining tissue fragments. The collected cell suspension was mixed with HBSS with 10% FBS to neutralize enzymatic activity and was kept on ice. The collected cellular fraction of each digestion were combined and washed in FACS medium (0.01% Na-azide 1% FBS in PBS). Cells were evenly distributed for each staining in a 96-multiwell plate. After a first wash in FACS media, cells were incubated during 30 min with the antibody cocktail (table 3) on ice and in the dark. Cells were washed twice in FACS media and transferred to FACS tubes. In order to exclude nonviable cells from the analysis, 0.5% of propidium iodide (P4170, Sigma-Aldrich) was added to the cell suspension 1-2 min prior to analysis. Fifty thousand events (of appropriate size and complexity) per staining were acquired in the cytometer FACS Canto II (BD Biosciences). Subsequent analysis and graphing were executed in FlowJo VX software.

For cell sorting, the same procedure was used with exception to the fact that cells were resuspended in Sorting Buffer (1mM EDTA, 25mM HEPES, 2% FBS in PBS) before being transferred to FACS tubes. Four cell populations were sorted using FACS ARIA II (BD Biosciences), according to CD90, PDGFRa (CD140a), Sca1 and CD44 expression. Thus, the cell signature of each population chosen was: 1) $Lin^-CD90^+CD140a^+CD44^+Sca1^-$; 2) $Lin^-CD90^+CD140a^+CD44^-Sca1^-$; 3) $Lin^-CD90^-CD140a^+CD44^+Sca1^{+/-}$ / $Lin^-CD90^+CD140a^-CD44^+Sca1^{+/-}$ / $Lin^-CD90^-CD140a^-CD44^+Sca1^{+/-}$ and 4) $Lin^-CD90^+CD140a^+CD44^+Sca1^+$.

Table 3. List of conjugated antibodies used in Flow Cytometry and specifications of the working dilution.

Antibody	Dilution	Reference
CD31-PeCy7 (Rat IgG2a)	1:100	25-0311, eBiosciences
CD45-PeCy7 (Rat IgG2b)	1:100	25-0451, eBiosciences
TER119-PE (Rat IgG2b)	1:100	116208, Biolegend
CD90.2-FITC (Rat IgG2b)	1:100	553013, BD Pharmingen
CD140a-APC (FL4) (Rat IgG2a)	1:100	135907, Biolegend
CD44-APC/Cy7 (Rat IgG2b)	1:100	103027, Biolegend
Sca-1-PE	1:100	108107, Biolegend

4.8 -   Neonatal Heart Digestion

Neonatal hearts (7 days post-injury/sham) were harvested and subdivided in apex, ventricles and atria. Then, each sample was cut into small fragments (approximately 2mm), before being flash frozen in liquid nitrogen, until further use. Then, fragments were thawed at RT and fixed with 4% paraformaldehyde (PFA) for 2 hours with stirring (100 rpm). Following fixation, fragments were digested with collagenase type II (Worthington, CLS-2) (3 mg/ml in HBSS) overnight at 37ºC (100 rpm) and mechanically dissociated until no fragments were detected. Additional digestions could be required depending on fragment original size and for that the collagenase solution was changed in 24h periods. In order to inactivate collagenase,

equal volume of HBSS with 10% FBS was added and kept at 4ºC until the digestion was complete. At this stage, cells can be stored at 4ºC in FACS media (containing 0.01% of Na-Azide) to prevent contaminations. These samples were used for cytospin immunofluorescence or for imaging flow cytometry.

4.9 -   Imaging Flow Cytometry

Cell suspensions were centrifuged at 300G for 10min and the cellular portion was then resuspended in FACS media (0.01% Na-azide 1% FBS in PBS) and permeabilized by 1X BD Perm/Wash™ Buffer during 15 minutes at RT. Incubation with primary (anti sarcomeric-α-Actinin (1:400, A7811, Sigma)) and secondary antibodies (Alexa Fluor 488 Donkey anti Mouse IgG (1:1000, A-21202, Invitrogen) lasted for 2 hours and 30 minutes on ice, respectively. Both antibodies were diluted in 1X BD Perm/Wash™ Buffer and incubations were separated by two washes with 1X BD Perm/Wash™ Buffer at 2000 rpm (240G). Finally, they were ressuspended in 1X PBS and kept at 4ºC until acquisition. Immediately before acquiring, cells were filtered (100μm cell strainer) and their nuclei was stained with 200 μM of DRAQ5 (5 mM, Biostatus).

CM morphometric analysis was performed using IDEAS® software. This software calculates several features of CMs (area, major axis, minor axis and aspect ratio) and allows mask creation (definition of a specific area) to access nuclei number. Thus, unfocused cells were promptly removed by eliminating cells with Gradient RMS smaller than 40 and debris and duplets were excluded by removing the objects with small area and high aspect ratio. To ensure that the analysis was focused on CMs, remaining events were plotted by the intensity of s-α-Actinin and DRAQ5 and double positives selected for subsequent analysis. Whenever the aspect ratio was smaller than 0.55, cardiomyocytes were classified as "Rod".

4.10 -   Immunocytochemistry

Cytospin immunofluorescence was performed following heart digestion. Isolated cardiac cells were plated onto glass slides using cytospin (Shandon Cytospin® 4, Thermo Scientific) and spun for 5 min at 130G. Cells were permeabilized with 0.5% Triton for 7 min and washed three times in PBS with 0.2% Tween. Then, cells were incubation for 2 hour with the following primary antibodies diluted in 1X PBS with 0.2% Tween: anti sarcomeric-α-actinin (1:400, A7811, Sigma) and anti-phosphorylated-histone3 (pH3) (1:800,#3377, Cell Signaling). These antibodies were used to stain CMs and karyokinesis, respectively. After three washes with 1X PBS with 0.2% Tween, 3 min each, samples were stained with the secondary antibodies for 30 min at RT, in the dark. Finally, nuclei were stained with DAPI for 10 minutes

and slides mounted in a PBS glycerol solution (1:9) with 2.5% n-propyl-gallate (Sigma-Aldrich) without DAPI.

4.11 -   Statistical Analysis

Data statistical analysis was performed with IBM SPSS Statistics 22 software. Shapiro-Wilk's test was used to evaluate if the data displayed a normal distribution. Samples considered as outliers were excluded from the statistical analysis at this point. Then, homogeneity of the sample was tested by Levene's test. These results defined the statistical test(s) used further. Normally distributed and homogeneous data were tested with parametric tests (independent samples T Test for 2 groups or one-way ANOVA for 3 or more groups). Tukey's post hoc test for correction of multiple comparisons was performed whenever significant differences were found between 3 or more groups.

Non-normal distributed and/or heterocedastic data were tested with non-parametric tests (Mann-Whitney U Test for two groups or Kruskal-Wallis one-way analysis of variance for 3 or more groups). Again, multiple comparisons were executed when 3 or more groups were considered statistically different by Kruskal-Wallis one-way test. The statistical significance level chosen for all statistical tests was p-value $(p)<0.05$. Results were shown as mean ± SD of the mean and are marked with one asterisk (*) if $p<0.05$, two (**) if $p<0.01$ and three (***) if $p<0.001$.

Chapter 5

Results

5.1 - Neonatal Hearts Do Not Fully Recover After Apex Resection

The robustness of the neonatal model of apex resection has been questioned since several technical variables have been reported to affect the injury outcome, namely the resection severity, the type of injury and even minor differences on the surgical procedure, which subsequently impact on the amount of scar formation [38, 41].

We established the exact same surgery protocol as described previously by Porrello *et al*. for apex resection in P1.5 C57Bl/6 neonatal mice, using the exposure of the LV lumen as a standardizing method for the resection size. The size of the lesion was determined immediately after resection, by the length of the heart vertical axis, normalized by the animal-body weight. The heart height/body weight showed a significant reduction of 13,8% when compared to sham-operated animals (p-value=0.011) (Figure 9). The low deviation of the resection size between injured animals showed reproducibility of the procedure. Furthermore, the extension of apex removal at our laboratory is comparable with other reports [32, 40, 41], legitimating further comparisons. The follow-up of the animals at 60dpr showed a statistical significant tendency for a persistent decrease on heart height/body weight of 13,08% (p-value=0.019) (Figure 9), which is indicative that apex-resected hearts do not undergo significant reestablishment of the resected region.

Aiming at detailed examination of histological alterations at the injury site, hearts were harvested and representatively sectioned and stained with Masson's Trichrome (Figure 10 (A)). The extent of the injury was estimated by determining the percentage of sections exhibiting cardiac fibrosis and/or elicit signs of tissue damage. Throughout the study we found a statistically significant reduction on the injury size of 28,1%, 42% and 58,3% between

0 and 21dpr (p-value=0.020), 21dpr and 60 dpr (p-value=0.018) and 0 and 60 dpr (p-value<0.001), respectively (Figure 10 (C)). Interestingly, although the heart is growing, the fibrotic scar maintains the same width throughout the injury response (Figure 10 (D)).
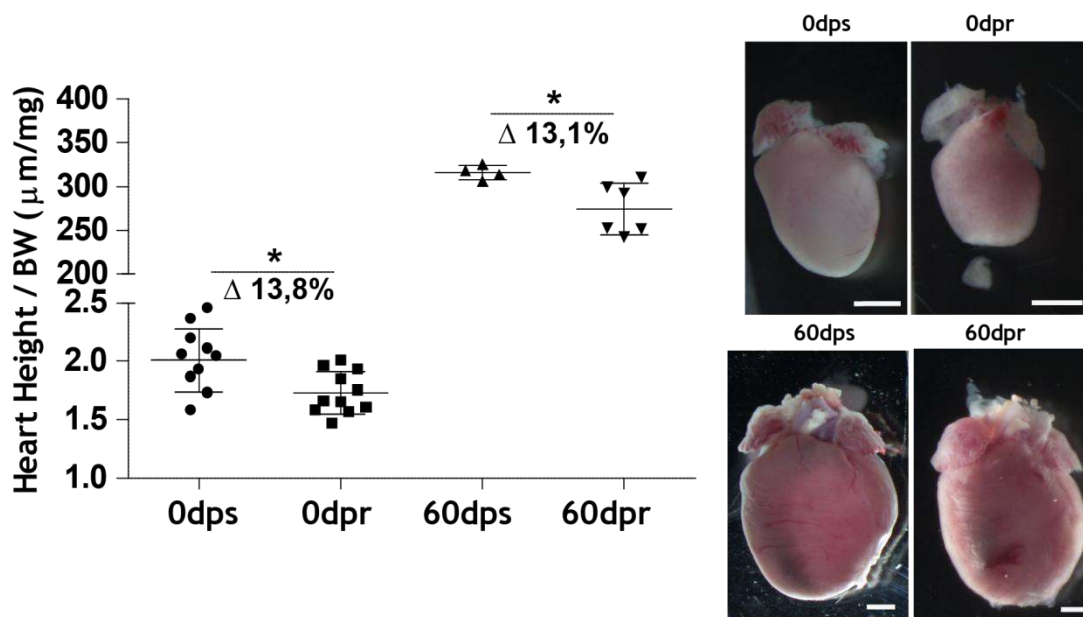

Figure 9. Assessment of the lesion size and heart recovery after surgery. The ratio heart height/BW was accessed at 0 and 60 days post-surgery (left), revealing surgical reproducibility and reduction of the cardiac long axis by 13% throughout the study. On the left panel, representative stereomicroscope images are shown for sham-operated and apex-resected hearts at the days of the surgery and 60 days after the procedure. Values are presented as means ± SD. Scale bar: 1mm. 0dps (n=11); 0dpr (n=11); 60dps (n=4); 60dpr (n=6).

Histological analysis of the injury site showed extensive deposition of cardiac fibrosis in the central sections of the heart, were the lumen was exposed after resection, whereas the surrounding apex region displays myocardial integrity. Of note, sham-operated hearts did not show any relevant histological and anatomical alterations (not shown), apart from epicardial surgical adherences, which is a common phenomenon to both experimental groups and relates to the surgical intervention. Importantly, at 60 days post surgery, all hearts analyzed displayed a transmural scar. This data contrasts with the results obtained at 21 dpr, a period in which a small amount of scattered myocardial fibrosis was present at the apex region (Chapter 2, Figure 6). Overall, these results are indicative that the apical tip, where extensive remodelling (collagen-rich scar) was found, does not regenerate efficiently (Figure 10 (B)). However, these results do not invalidate the hypothesis that the apex region adjacent to LV free wall and to the intraventricular septum may have undergone regeneration, as fibrosis was restricted to the epicardium and not found within the myocardium of these areas (Figure 10 (B), left).

(Neo)vascularization, a requirement for regeneration, was accessed by semi-automatic quantification of CD31 (endothelial-associated marker) expressing cells (CD31^{+}) 60

days following surgery. We found that vascularization was not impaired, being slightly but significantly increased in comparison to sham operated animals. Restricting the analysis to the apex region, revealed that the number of CD31$^+$ cells per area was increased in central/fibrotic sections when compared with peripheral/non-fibrotic ones in both injured (33%, p-value=0,005) and sham operated animals (18%, p-value=0,04). Consistently, apex resected hearts showed a statistical significant increase in the percentage of CD31$^+$ cells in central (14,9%, p-value=0,09) and in peripheral sections (30,8%, p-value=0,014) when compared to surgical controls (Figure 10 (E)). Interestingly, in the remote area (above papillary muscles) of central sections the trend for an increased neovascularization persists after apex-resection (Figure 10 (F)), although statistical significance was not obtained.

5.2 - Cardiomyocyte Proliferation Is Activated Upon Neonatal Apex Resection

One fundamental feature of the neonatal mouse resection model noted by Porrello *et al.* is an increase of CM cell-cycle reentry upon injury. In contrast, Andersen *et al.* did not observe the same mechanism in resected hearts. To test whether resection results in an augment in cell cycle activity, cardiomyocytic proliferation was automatically quantified on cryosections using an algorithm that co-localizes α-actinin, DAPI and pH3 staining, which label CMs, nuclei and karyokinesis, respectively (Figure 11 (A)). When evaluating the myocardium below the papillary muscle, CM proliferation occurs at a significant higher rate in the apex resected group when compared to the sham group (p-value=0.001), representing a fold-increase of 2.44 (Figure 11 (C)).

To reinforce this idea, a similar analysis was performed on cytospins of isolated CMs (Figure 11 (B)). Accordingly with the previous analysis, proliferative CMs were identified through the co-localization of of s-α-Actinin, DAPI and pH3 staining in the same cell. In this case, injured hearts have a greater fold-increase (3.45) in proliferating CMs, yet this result did not reach statistical significance (p-value=0.149) (Figure 11 (D)). This analysis will be repeated to increase the biological replicates and strength statistical robustness.
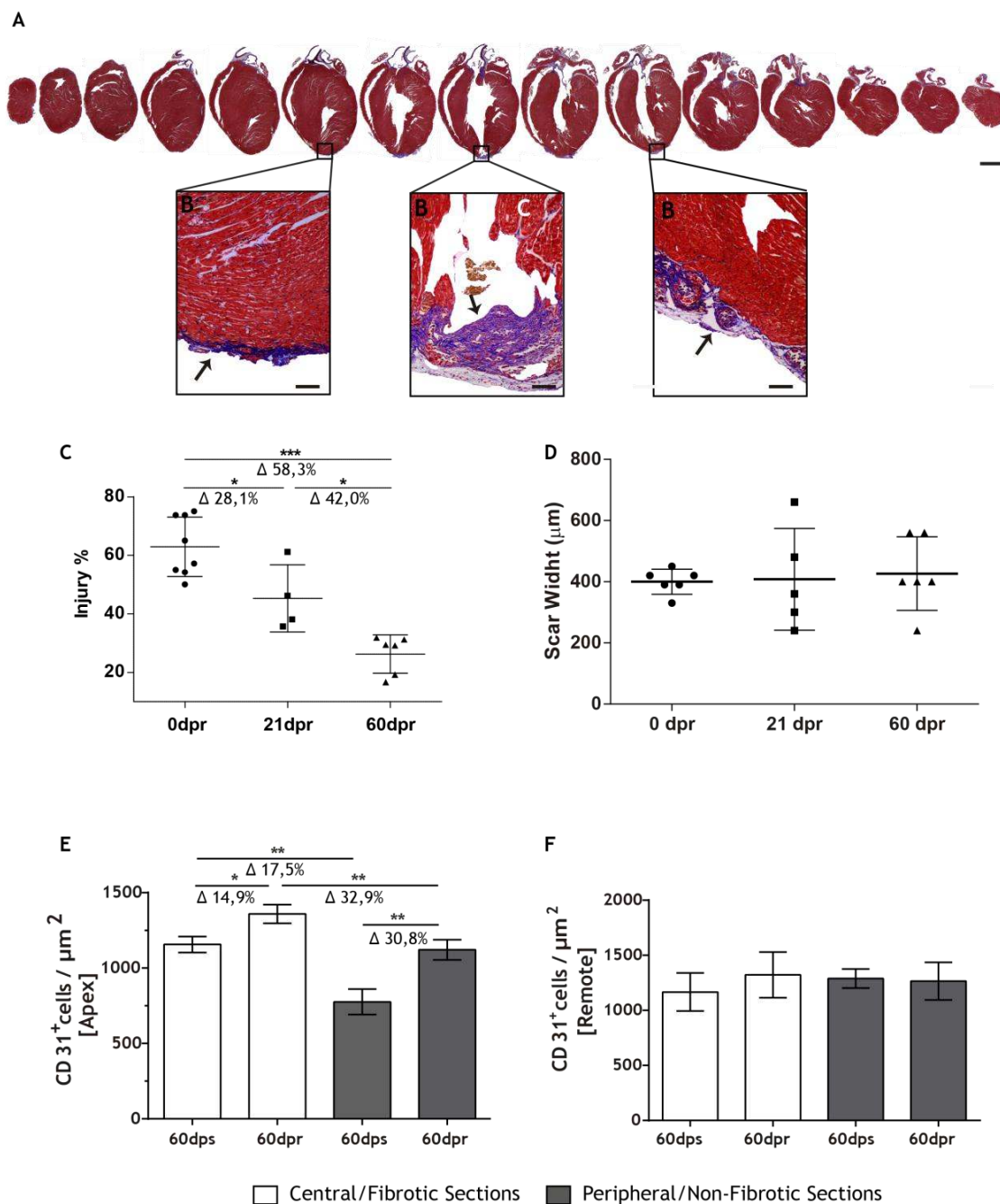
Figure 10. Characterization of the neonatal cardiac injury response. (A) Masson's Trichrome representative sections of apex-resected hearts at 60 days post-apex resection. Scale-bars: 2 mm **(B)** High power images of Masson's Trichrome focusing the injury site with arrows highlighting collagen deposition. Scale bar: 100 μm. (C) Percentage of heart sections displaying signs of lesion throughout the study (0, 21 and 60 days post-apex resection). Although the heart is not fully recovered after 60 days post-apex resection, the injury representativeness decreases, however, scar width is maintained through time (D). Values are presented as means ± SD. 0dpr (n=8); 21dpr (n=4); 60dpr (n=6). (F-G) Neovascularization at 60 days following injury. The number of CD31^{+} cells per area was accessed in the apex (E) and remote zone (F), demonstrating that in apex-resected hearts, vascularization was not impaired. Values are presented as means ± SD. 60dps (central n=12; peripheral n=6); 60dpr (central n=14; peripheral n=11).

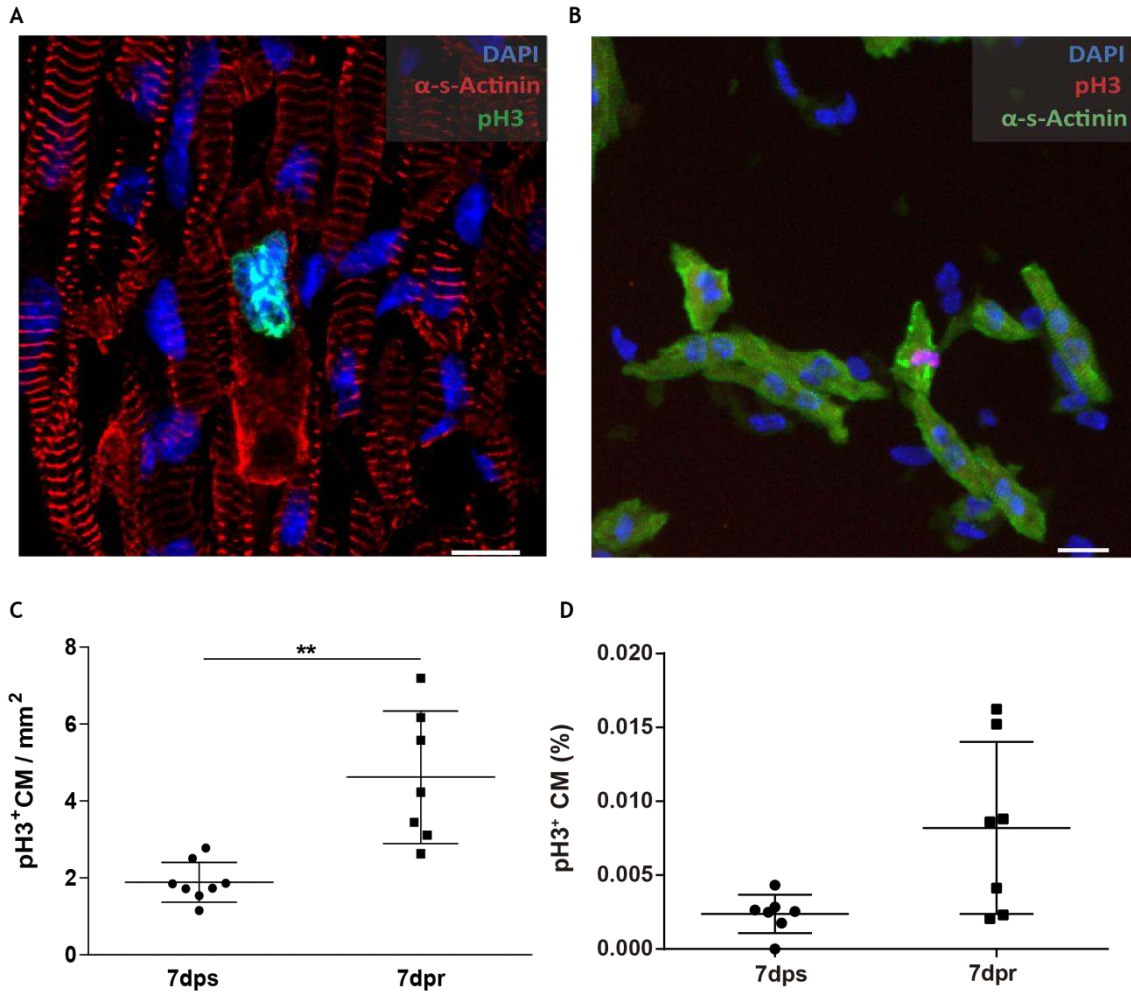**Figure 11. Proliferative behavior of CMs at the injury site.** (A-B) Representative proliferative CMs of the apex region at 7days after surgery, in situ (A) and following CM isolation (B). Scale bar: 10μm. (C-D) CMs proliferation is significantly increased on the apex of injured animals when compared to sham-operated controls at 7 days post-surgery. (C) cryosections (7dps n=8; 7dpr n=7); (D) cytospin (7dps n=7; 7dpr n=7). Values are presented as means ± SD.

The loss of CM proliferative potential is commonly attributed to the development of a terminally differentiated phenotype that is characterized by the presence of the differentiated sarcomeric cytoskeleton and binucleation [73]. In order to assess whether after resection the rate of CMs displaying an immature phenotypes was increased, morphometric analysis of the CMs was performed (Figure 13). Hence, when the aspect ratio is bigger than 0.55, CMs were classified as "round", correlating with a more immature phenotype, otherwise CMs were classified as rod (mature phenotype). At 7 days post injury, imaging flow-cytometry analysis revealed that round CM were increased by 26,9% and 111% in the apex and remote areas, respectively, of the apex-resected group (p-value = 0.030 and 0.012, respectively). Interestingly, this morphometry correlates with a more immature CM

phenotype, which is thought to be more proliferative [126]. Nonetheless, rod-shaped CMs were always the predominant population among the total population of CMs (Figure 12 (A)). Intriguingly, the global area of CM was statistically higher in the apex of injured animals (Figure 12 (B)). In accordance, the area of mature CMs (rod-shaped) in apex-resected hearts is increased by 21,6% (p-value 0,021), which could explain the increase in global CM area. In the remote zone an opposite trend was observed since rod-shaped CM were 13,9% smaller (p-value=0.037) (Figure 12 (C)). These results are indicative of a local compensatory CM hypertrophy in the border zone of the injury, whereas at remote regions CMs are smaller.
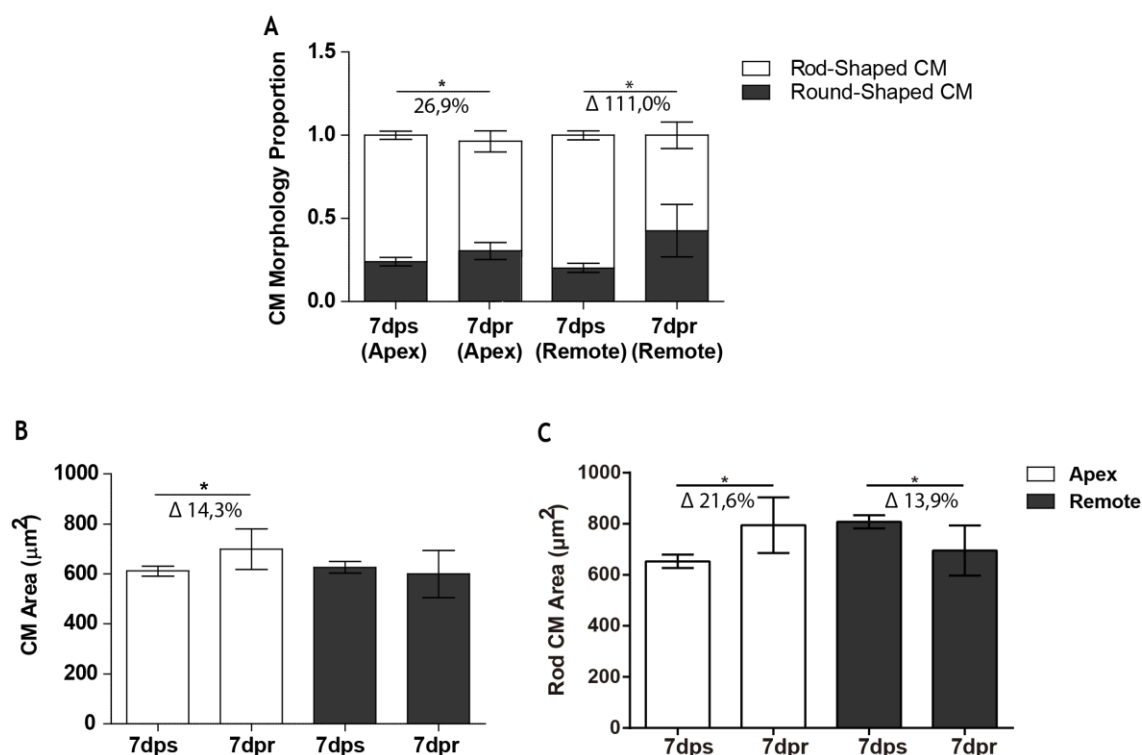
Figure 12. CM morphometric parameters at 7 days following surgery. By imaging flow cytometry, CM morphology was accessed showing an increase on the number of immature CMs (A). The global CM area was increased in the apex (B) and these are associated to a bigger area of rod-shaped CMs (C). Values are presented as means ± SD .7dps (n=7); 7dpr (n=7).

To assess whether this hypertrophic phenotype was maintained throughout the study, the surface area of cross-sectioned CM was assayed at 60 days after apex resection. In fact, no signs of hypertrophy were detected and CM cross-section area was considerably smaller in injured hearts both in apex and remote zone when compared to sham, although statistical significance was only reached in the remote area (Figure 13 (A)). Further analysis revealed that CM surface area in the apex diminishes especially in areas adjacent to the injury (p-value=0.044) whereas, in lateral/peripheral sections, the same tendency is verified although no statistical significance is achieved (Figure 13 (B)).
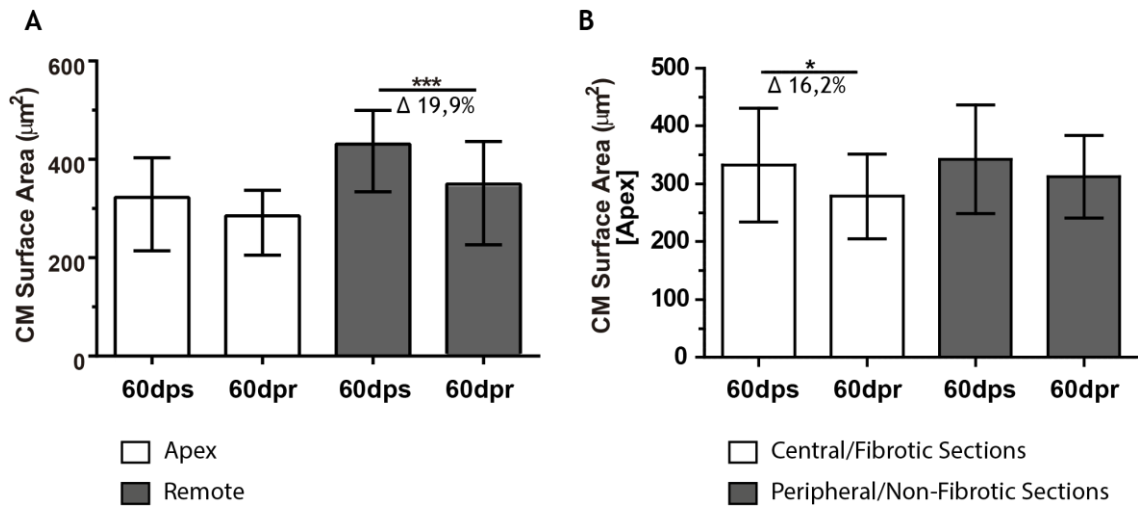
Figure 13. CM surface area quantification. CM surface area of injured mice, manually quantified in histological sections, showed a decrease when compared to sham operated animals in apex and remote areas (A). 60dps (n=28); 60dpr (n=64). Within the apex (B), a notorious difference was observed in CM of central/fibrotic sections between groups. 60dps (central n=14; peripheral n=14); 60dpr (central n=32; peripheral n=26). Values are presented as means ± SD.

Considering that a decrease on CM size may impact on efficient intercellular communication, we evaluated the expression of Cx43, the main cardiac gap junction protein, on the apex area of apex-resected and sham-operated animals. An evident subexpression of this protein in injured hearts was observed, mainly in apex regions where collagen deposition in the intercellular space was more perceptive (Figure 14).

Figure 14. Representative images of Cx43 expression-pattern 60 days after surgery. The apex of resected hearts clear down regulation of this gap junction protein. Scale bar: 1 mm. 60dps (n=3); 60dpr (n=6).

5.3 -   Dynamic Deposition of Extracellular Matrix Instructs the Myocardium Upon Injury

Several evidences support that the production of ECM is one of the mechanisms activated during cardiac regeneration in lower vertebrates [127]. To address in detail the extracellular and cellular dynamics aforement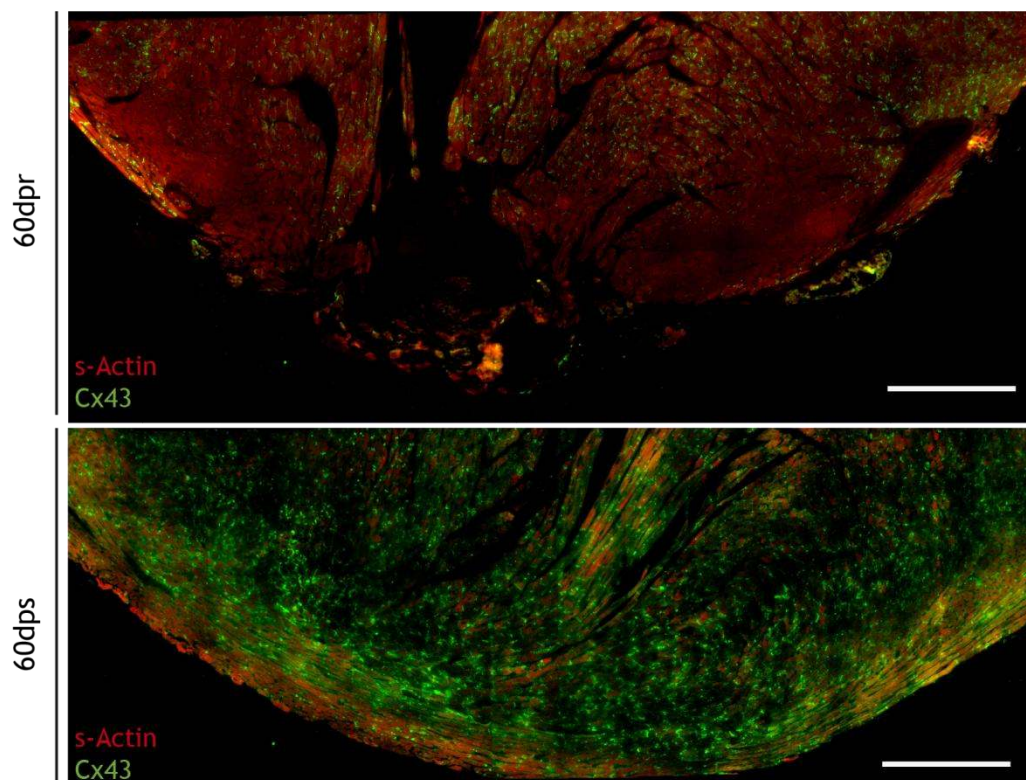ioned in the Preliminary Data section (Chapter 2), we focused primarily on the deposition of Fn and Tn-C, which we have shown to be upregulated following apex-resection (Figure 7).

The deposition of ECM was assayed at 48h and 7 dpr, i.e. in the peak of inflammation and fibroblast proliferation, respectively (Figure 15). At an early stage (48 hours post-apex resection), the deposition of Fn and Tn-C is associated with hematopoietic cells (CD45 expressing cells) as, by immunofluorescence confocal microscopy, we are able to detected a co-localization of these three markers (Figure 16). In contrast, at later stages (7 dpr), Fn and Tn-C become co-localized with myofibroblasts (α-SMA$^+$ expressing cells), indicating a shift in the cell types responsible for the production and deposition of these two ECM components (Figure 15). Considering the pattern of Fn and Tn-C deposition, although largely overlapping, Fn has a broad expression pattern throughout the injury site than Tn-C, which is confined to the boundaries between injured and healthy tissue (Figure 16).
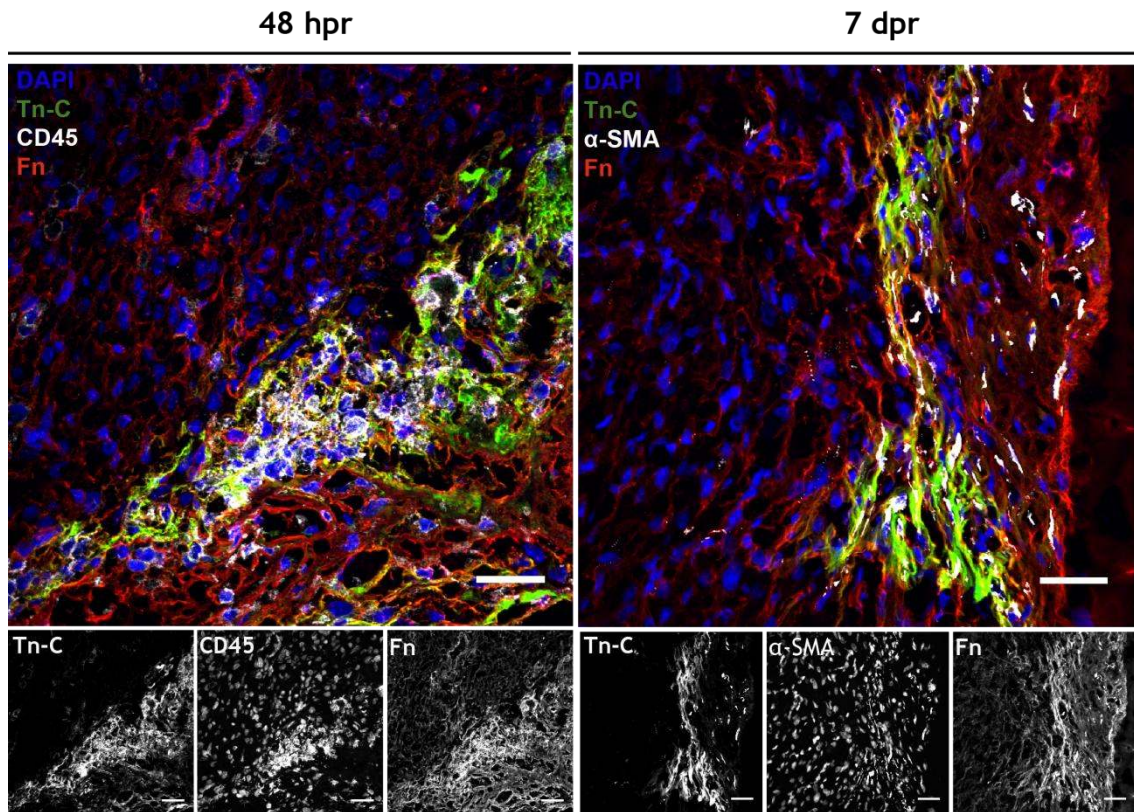
Figure 15. Cellular source of Fn and Tn-C at the injury site. Representative immunofluorescence images at injury site, 48h and 7 days following apex resection, demonstrating a shift in the cellular source of both proteins. Scale bar: 30 μm. 48hpr (n=4); 7dpr (n=4).
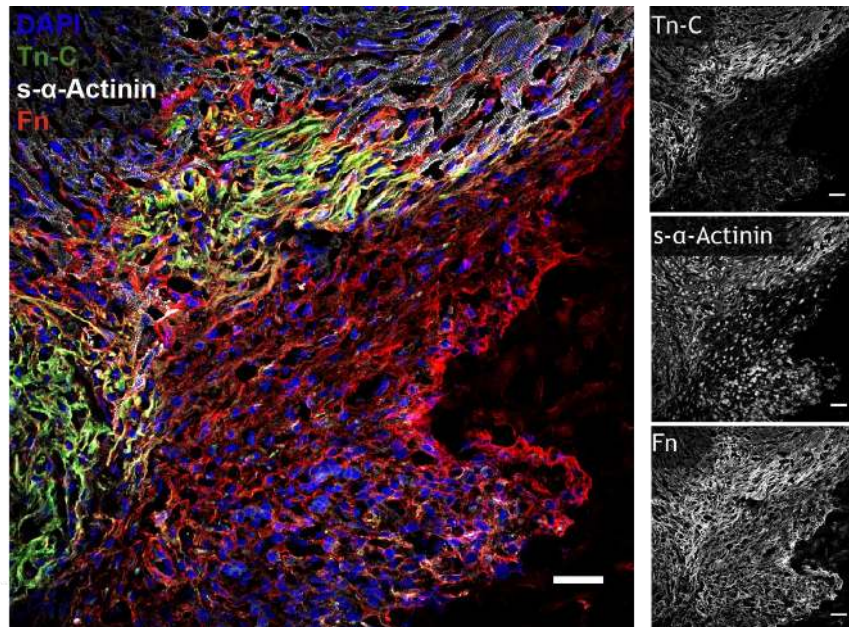
Figure 16. Fibronectin and Tenascin-C have distinct deposition patterns. Representative images of Tn-C and Fn deposition in the apex, 7 days post-apex resection. Co-localization of these proteins is observed, however Fn presents a more disperse expression pattern when compared to Tn-C, which is restricted to the margin of the injury. Scale bar: 30μm. (n=4)

We then hypothesized that ECM deposition would play an instructive role at injury site by promoting higher levels of cardiomyocytic proliferation and/or CM migration to the injury site. Once the proliferation of CMs is up-regulated at 7 days post-apex resection (Figure 11) we focused on this time-point. Mitotic CMs were predominantly found in the vicinity of these two extracellular matrix components and, importantly, CMs exhibit the expression of CD29 (also known as integrin-β1), an important integrin chain that mediates cell-matrix interactions [104] (Figure 17).
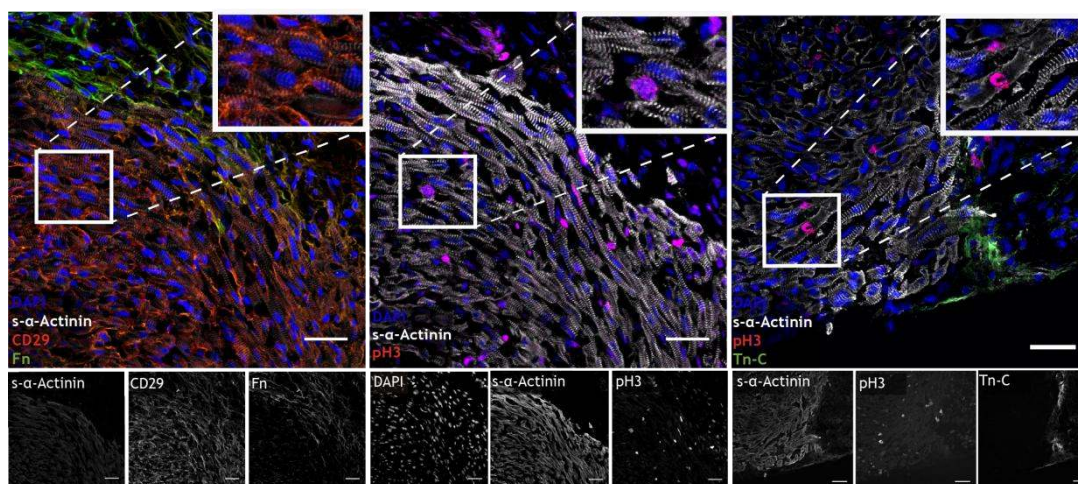
Figure 17. The instrutive role of ECM. Representative images of mitotic cardiomyocytes (s-α-Actinin[+]pH3[+]) in the vicinity of extracellular matrix deposition (Fn and Tn-C) at 7 dpr. Analysis of adjacent sections showed that proliferative CMs express CD29 and are associated with Fn-rich regions. Scale bar: 30 μm. (n=4)

5.4 -   The Role of Cardiac Fibroblasts following Neonatal Cardiac Injury

Considering that, after the peak of inflammation, Tn-C and Fn are mainly produced by myofibroblasts (Figure 17) and that collagen is being deposited the core of the lesion (Figure 10 (B)) at later time-points after apex-resection; we postulated that fibroblasts are activated during this process. To unveil their intervention in response to injury, flow cytometric profiling of these cells was performed. The fibroblast population was herein defined by the expression of CD90 (Thy-1), a well-reported marker of cardiac fibroblasts [117], after exclusion of endothelial (CD31), hematopoietic (CD45) and erythroid cells (TER119).

Among the markers ascribed in the previous ontogenic characterization (Figure 8 Chapter 2), we decided to ascertain CD44, Sca1, CD105 (Endoglin), CD106 and CD140a (PDGFRα) expression levels upon apex resection. CD105 is an accessory glycoprotein of TGFβ

receptor complex that modulates the cell response to several TGFß superfamily ligands, namely TGF-ß1. This signalling pathway promotes type I collagen synthesis and fibrosis [128]. CD106 (also known as vascular cell adhesion molecule 1-VCAM1) is involved in angiogenesis, cardioprotection and also in the initiation of the inflammatory process [20, 129].

At 7 post-surgery, the percentage of CD90$^+$and CD90$^+$CD106$^+$ cells was not different between injured and sham-operated mice. In contrast, a significant increase was observed in the frequency of CD90$^+$CD44$^+$ and CD90$^+$Sca1$^+$ (p-value=0.27, and 0.13, respectively) whereas CD90$^+$CD105$^+$ population significantly decreases (p-value=0.016). Additionally, considering the proliferation in the stromal compartment (CD31$^-$CD45$^-$, TER119$^-$), no statistically significant differences were found on Ki67 expression levels between injury and sham-operated animals. However, the percentage of Sca1$^+$ proliferating cells (p-value<0,001) almost doubled in injury conditions (Figure 18).
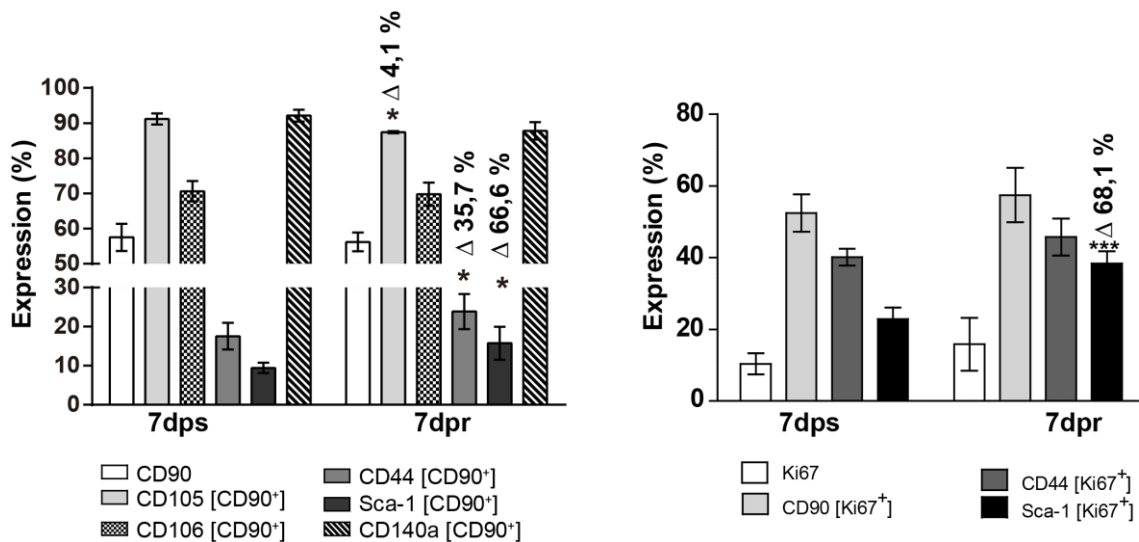
Figure 18. Phenotypic characterization of cardiac fibroblasts 7 days after apex-resection. CD90 expression profile (left) and proliferation (Ki67, right) of the stromal compartment (CD31$^-$CD45$^-$TER119$^-$) was investigated post-apex resection and post-sham surgery (left). 7dps (n=6); 7dpr (n=5).

Given the extensive overlap between these markers, we decided plot the same data resorting to Venn Diagrams, which allows comparison of three markers simultaneously. Thus and looking inside the cardiac fibroblast compartment (CD90$^+$ cells), we display the co-expression of CD140a, CD44 and Sca1 (Figure 19). In this representation, the main population differences between sham and injured hearts reside on the increase of CD90$^+$CD44$^+$ (red), CD90$^+$CD44$^+$CD140a$^+$ (purple) and CD90$^+$Sca1$^+$CD44$^-$CD140a$^-$ (yellow), and decrease on CD90$^+$Sca1$^-$CD44$^-$CD140a$^+$ (blue) cardiac fibroblasts. However, only CD90$^+$Sca1$^+$CD44$^-$CD140a$^-$

population reached statistical significance (p-value=0.036) whereas $CD90^+Sca1^-CD44^-CD140a^+$ obtained a p-value of 0.059.

Based on this information, we strategically sorted 4 populations with the most distinct expression profiles (see Material and Methods Cell Sorting). qPCR of these populations will be valuable to detect differences at the transcriptomic level which could translate in different roles on the cardiac injury response. This experiment will be performed in the near future, and therefore this results will be out of the scope of the herein dissertation.

Figure 19. Venn Diagrams of the stromal heart populations 7 days following injury. The major differences noticed were in CD90+CD140a+ (blue), CD90+CD44+CD140a+ (purple) and CD90+Sca1+ (yellow) populations. 7dps (n=6); 7dpr (n=5).

Chapter 6

Discussion

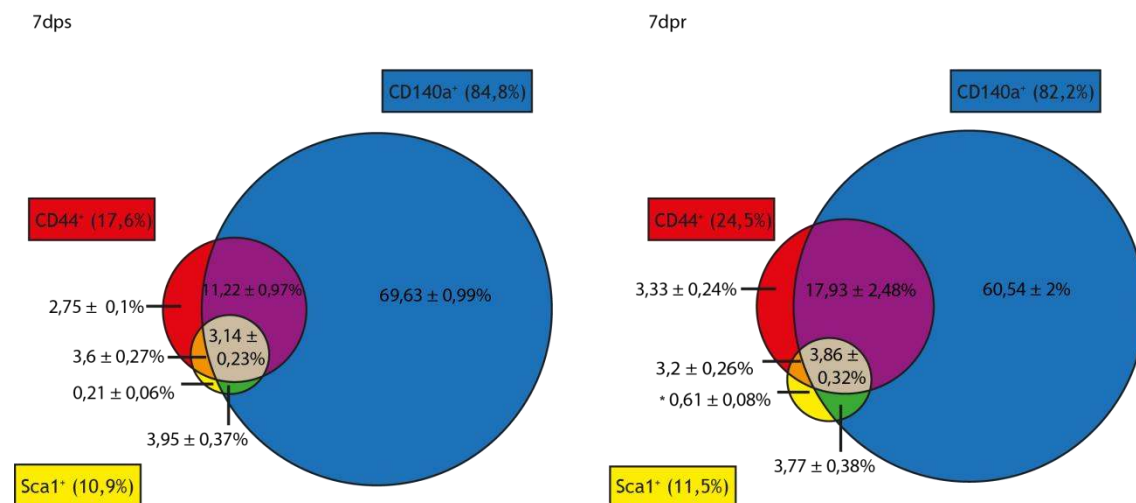Cardiovascular diseases are the leading cause of death worldwide, representing 30% of global mortality. Unfortunately, available projections show that this tendency will persist and, currently, the only long-term effective therapy for heart failure is cardiac transplantation [1]. Hence, the development of novel therapies to re-establish the myocardium or, at least, to improve cardiac repair following injury are mandatory.

Looking into heart evolution along phylogeny, several evidences suggest the existence of a compromise between adaptation and regenerative capacity [2]. Albeit mammalian heart has been considered genuinely unable to regenerate upon injury, a ground-breaking discovery reported that murine hearts retain an intrinsic yet transient regenerative capacity. Hearts from 1-day-old mouse were reported to fully regenerate from apex resection within 21 days. In contrast, 7-day-old mice lack regenerative capacity and hearts develop a reparative response, originating a collagen-rich scar, and therefore, compromising cardiac function [3]. This exciting data brought a valuable platform to dissect molecular networks governing cardiac regeneration and thus propelling the design of new cardiac therapies. Regardless of apex-resection injury model has been replicated in other laboratories, cited over 300 times and corroborated by distinct injury models [4-9], in 2014, Andersen et al. refuted the existence of neonatal cardiac regeneration, reporting a massive collagen deposition even when the lesion was inflicted in the first week of life [10]. A consensus on the field is still missing although independent studies have already committed in determining the basis for such different outcomes. In this sense, herein work aims to understand which reparative or

regenerative features prevail after apex resection, focusing particularly on the dual role of cardiac fibroblasts and ECM deposition.

Neonatal apex resection model was successfully established in our lab however technical differences, in comparison to previous studies, should be considered. In the herein work, surgery was performed in P1.5 C57BL/6 neonates, i.e. 36h post-birth. Porrello *et al.*, analysed P1 ICR-CD-1 heart as such, and assuming that they performed the surgery in the first 24h post birth, our injury is set half a day later, which is still within the reported regenerative time window. Moreover, distinct strains might have different responses to injury and C57BL/6 mice have been considered non-healers [11], however, Andersen *et al.* did not found any strain-specific responses between this strain and the ICR-CD-1.

In resemblance to Porrello et al., we used the exposure of the left ventricle lumen, as a standardizing method for the resection size. This approach resulted on a reproducible outcome as a 14% reduction is consistently obtained in heart height/body weight ratio (Figure 9). Even still, the severity has been assayed by different methodologies (ventricle weight, surface area and heart weight/body weight) across laboratories, jeopardizing direct comparison of data. In our hands, the injury extension is within the range mentioned in the available reports. In spite of our best efforts, we failed to weight accurately the LV of the animals, as the resected tissue weight is within the deviation of our precision weighing scale (0.01 mg). Indeed, C57BL/6 mice are smaller than the ICR-CD-1, and therefore, to attain a similar resection size, the weight of the resected tissue is smaller, limiting quantification. Additionally, the survival rate of apex-resected animals to the surgery (≈85%, Figure 4) is similar to other reports, supporting the successful establishment of the injury-model. Notwithstanding, at 60 days after surgery the heart height/body weight ratio variation between groups suggests that the injured heart did not recover the apex. Although the scar width is maintained throughout time, its representativeness in the heart diminished. This could be justified by the growth of the heart; however, we cannot disregard the possibility of partial tissue reestablishment through activation of regenerative mechanisms. At the histological level reparative mechanisms are evident at 60 dpr since a full-thickness scar is formed in the centre of the apex, resembling a small aneurysm (Figure 10 (B)). Interestingly, although interstitial collagen deposition is evident in apex-resected hearts at 21dpr, none of the analysed hearts displayed a full-thickness scar. This evidence is indicative that from 21 to 60 dpr, myocardial fibrosis expanded to form an aneurism-like structure, whereas in the adjacent regions, where disperse collagen was identified, the myocardium was mainly restored. This scenario is consistent with the activation of CM proliferation in the border-zone of the injury, i.e. in the LV and interventricular septum (IVS) myocardium, which may provide gradual replacement of peripheral scar tissue by newly contractile myocardium. Clearly, the augmented CM proliferation (Figure 11) is not sufficient to fully recover the

myocardial wall in the centre of the apex. Hence, these results contrast to the original description of neonatal apex regeneration, in which fibrosis was reported as non-evident [3]. The reestablishment of the new vasculature is also a pivotal mechanism for heart regeneration as otherwise, blood supply to the damaged area is ineffective/absent [12]. Interestingly, no impairment on the neovascularisation was observe throughout the heart, and therefore the regenerative mechanisms underlying vessel formation are efficiently activated following apex-resection rendering this injury-model as a good system to study cardiac neo-angiogenesis. Moreover, the reestablishment of the vasculature levels occurs even in the fibrotic zone contrasting to the injury response upon AMI in the adult heart [13]. The innate capacity for angiogenesis reactivation in neonatal hearts may rely on the immune system once it was demonstrated that monocytes/macrophages influence neovascularization during cardiac regeneration. Interestingly, following monocytes/macrophage ablation, cardiac regenerative capacity is impaired mainly by an insufficient neovascularization [14]. Our results concerning revascularization of the resected area clearly contrast to the Andersen et al. report, which demonstrated that the damaged apex comprises modest vascularisation [10]

The CM cell cycle re-entry was the first postulated mechanism for the restoration of myocardial tissue after apex resection [3]. Nevertheless, within the controversy settled around neonatal cardiac model, CM proliferation was refuted by Andersen *et al.* [10]. High-content imaging analysis showed that at 7 days post-surgery, CM proliferation was significantly increased in the apex region, when compared to sham operated controls. Reinforcing this premise, a different analysis procedure (manual quantification on cytospin) revealed the same tendency. Although, no CM lineage tracing has been performed in the herein MSc Thesis, the hypothesis that best suits our data is that newly formed CMs drive from pre-existing ones, once we successfully show an increase in mitotic CMs with sarcomere disassembly (Figure 11), characteristic of dedifferentiation events [15]. Nevertheless, we cannot exclude the possibility that stem or progenitor cells also contribute to this process.

Interestingly although both regenerative and reparative mechanisms have been activated and hearts are not fully restored at 60 dpr, we did not found any evidence of compensatory hypertrophic growth. On the contrary, injured hearts displayed smaller CMs when compared to sham operated animals. Nevertheless, at 7 dpr, rod-shaped CMs display increased areas when compared to the respective sham-operated control. We hypothesized that this is a transient, yet necessary response to promote wound closure once hypertrophic CMs are only detected in the apex region. Curiously, the area variation levels between 7 and 60 dpr are approximately equal to the previously found at 7dpr (≈15%), which indicates a recovery of the CM morphometric parameters at latter time-points.

AMI causes an increase in myocardial resistivity and a decrease in conduction velocity that culminate in an arrhythmic behavior [16]. Cardiomyocytic gap junctions are determinant in this process and in prolonged hypoxia environments, downregulation and internalization of Cx43 at gap junctions occurs [17]. Our results showed a downregulation of Cx43 on injured hearts, and although the electrical activity of the hearts at 60 days post-surgery was not evaluated, this information suggests impairment in the conduction system. Moreover, subexpression of Cx43 occurs in areas where the deposition of collagen is notorious. Interestingly, a study demonstrated that a reduced expression of Cx43 promote fibrosis during pathophysiological condition [18].

To dissect the biological players involved in the injury response, the ECM dynamics was characterized. In our preliminary data we showed that the neonatal injury response at P1.5 involves, in an initial stage, the formation of a blood clot and consequent recruitment of inflammatory cells. Between 5 and 7 days post-surgery, the inflammation enters in its resolution phase, which is concomitant with the appearance of fibroblasts and myofibroblasts. Finally, 21 days following injury, the myocardium partially recovers its expression pattern, suggesting heart recovery at some extent (Figure 5). Interestingly, during this process, ECM is reshaped, which is highlighted by Fn and Tn-C expression. These ECM proteins are significantly upregulated from 48hpr until 21dpr. Curiously, there seems to be a double origin for their deposition, as primarily it is associated with hematopoietic cells and latter with myofibroblasts. Although Fn and Tn-C are derived from the same cellular sources, their deposition patterns are distinct at 7 dpr. Fn is a known mediator of several cellular interactions such as migration, proliferation and angiogenesis, being widely expressed in healthy myocardium [19]. On the other hand, Tn-C is a counter-adhesive glycoprotein and is able to promote cell proliferation, migration or regulate cell attachment [20]. Contrarily to Fn, this protein is barely detected in the normal adult heart but transiently expressed when associated with tissue remodeling [21]. In zebrafish, injury-mediated Fn and Tn-C deposition is essential to promote CM migration to the injury site [22, 23] whereas in cultured mammalian CMs, Fn induces proliferation through β1 integrin (also known as CD29) [24]. In newt, alongside with hyaluronic acid, both Fn and Tn-C promote CM cell-cycle reentry [20]. Altogether, the accumulation of these molecules in the damaged myocardium likely recapitulates, to a limited extent, the regenerative response of lower vertebrates, improving cell migration to the injury site. However, in adult human hearts, Tn-C and Fn expression is observed during wound healing upon myocardial infarction, originating a transient matrix necessary for further organization of other proteins like collagen [25].

Since Fn and Tn-C have also been associated with CM proliferation [20], we hypothesized their involvement with the increased proliferation of CM after apex-resection. To this end we aimed to co-detect these markers with proliferating CMs. However, as our Fn and pH3 antibodies were produced in the same species, we were not able to simultaneous

detect the expression pattern these two proteins. As an alternative strategy, we used consecutive sections (Figure 17) for each immunostaining. Proliferating CMs were not found on Tn-C rich areas, which might be explained due to the counter-adhesive properties of this protein. Contrarily, higher CM mitotic levels were found in the vicinity of Fn deposition at the injured area, and importantly, proliferating CMs express CD29 (integrin ß1), which may be one of the element mediating cell-matrix interactions.

The resolution of cardiac injury encompasses microenvironmental alterations that seem to trigger fibroblast activation and proliferation. Although the total amount of CD90^{+} fibroblast was not altered, within the CD90 compartment, we observed a statistical increase in the percentage of cells expressing CD44 and Sca1. This data is anticipated since CD44 and Sca1 are upregulated in the injured adult heart, being associated to the activation of fibroblasts and as a progenitor-like phenotype, respectively [26, 27]. Interestingly, CD105^{+} (aka endoglin) cardiac fibroblasts were downregulated in injured hearts when compared to sham operated animals. In adult hearts, reduced CD105 expression attenuates cardiac fibrosis and preserves left ventricular function by limiting TGFß1 signaling and type I collagen synthesis by cardiac fibroblasts [28]. The observed reduction on CD105^{+} cardiac fibroblasts may suggest that cardiac fibroblast after apex resection change phenotype towards the production of less collagen at 7 dpr, a period in which CM proliferation occurs. Furthermore, considering the proliferative rate of these populations, only Sca-1^{+} cells proliferate consistently following injury. On the other hand, the evident increase on CD44^{+} cardiac fibroblasts, is more likely a product of phenotypic alterations resultant from cardiac fibroblast activation and differentiation in myofibroblasts. Despite that the obtained differences on cardiac fibroblast dynamics are subtle; their frequency is most likely diluted since the cytometric analysis was performed with the whole heart rater that with the damaged area. We developed a sorting strategy to isolate cells that have a more dissimilar phenotype comparing to sham, in order to study their transcriptomic profile. Thus, based on their transcriptome we aim to distinguish populations of fibroblasts and correlate their expression profile with a more regenerative or reparative profile.

Overall, our results suggest that upon apex-resection murine hearts undergo neomyogenesis, ECM remodelling, neovascularisation and do not show signs of hypertrophy or cardiac dysfunction. Intriguingly, our results do not fully replicate any of the previous reports. At 21 days following injury, Porrello *et al.* reported full restoration of myocardium with minimal fibrosis whereas Andersen *et al.* described the accumulation of a massive scar in the resection site and no evident signs of CM proliferation. Indeed, at histological level, our results resemble more Andersen *et al.* although with less robust collagen formation.

However, a detailed analysis of the injury response unveils similarities with Porrello *et al.*, namely higher CM proliferative rates and no evidences of hypertrophy. Concerning the lack of reproducibility among reports, the lack of representativeness on the analysed tissue sections has been appointed to be the origin of such discrepancies [29-31]. Thus, a diminished representativeness can mask the injury site, misleading the final interpretation. Porrello *et al.* only sliced 140 section of 5μm per heart whereas Andersen et al. obtained 820. To address this technical limitation we have performed representative sections of the whole heart with constant intervals between each section, thereby increasing robustness of analysis. Furthermore, the duration of the previous studies (21d) might have been insufficient to address the final outcome of the heart injury response once the expansion of the myocardial collagen-rich scar occurs from 21d to 60d. An important limitation of the herein work is the lack of functional results at 60d post-surgery, which constitute one of the experiments to address in the near future (Table 4).

Chapter 7

Conclusion

The herein work discriminates the cellular and extracellular dynamics of the neonatal heart injury response, until 60 days following surgery (Figure 20). We demonstrate that immediately after injury, a blood clot is formed to prevent extensive hemorrhage, which is also the origin of inflammatory cells. Then, ECM remodeling takes place, mainly by the overexpression of Fn and Tn-C, which may be important to promote CM proliferation and/or migration towards the injury area. Although CMs re-enter in the cell cycle, CM turnover is insufficient to ensure restoration of the lost tissue. Thus, fibroblasts and myofibroblasts orchestrate the establishment of a fibrotic scar in the center of the lesion, promoting cardiac fibrosis, which until 21dpr did not affect systolic function.

Interestingly, following apex-resection we report both regenerative (neomyogenesis, neovascularization) as well as reparative mechanisms (myocardial fibrosis) and therefore this injury-model constitutes a valuable tool to dissect the switch between both mechanisms.

During neonatal injury response cardiac fibroblasts seem to have a dual role. Hence, cardiac fibroblasts are responsible for the production of regeneration-associated proteins (e.g. Fn and Tn-C), however at later time-points they acquire a fibrogenic phenotype, characterized by the production/deposition of collagen. Hence, further studies are required to ascribe the role of the different fibroblast populations following cardiac injury. We have established the grounds for the transcriptomic analysis of different cardiac fibroblast subsets by FACS-sorting the main populations altered following apex-resection.

Overall, the results herein described represent a conciliatory perspective on neonatal cardiac response to injury. Both regenerative and reparative mechanisms seem to be

activated upon injury, although the regenerative capacity reveals to be insufficient to completely restore the neonatal, being overwhelmed by repair.
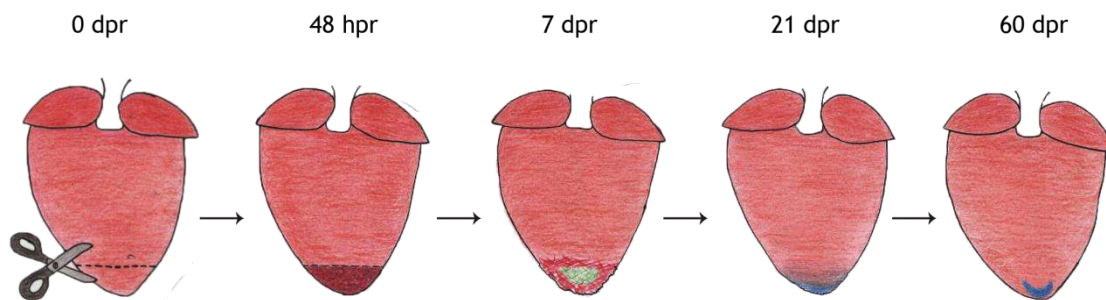

Figure 20. Proposed model of neonatal heart injury response. After apex resection, a blood clot is formed, initiating the inflammatory response through infiltration of hematopoietic cells. Gradually, ECM remodeling occurs by overexpression of Fn and Tn-C, initially associated with hematopoietic cells and afterwards with fibroblasts/myofibroblasts. While the microenvironment induces CM migration and proliferation from the neighbouring myocardium to the apex, at the central region, where the lumen was exposed, cell repopulation is insufficient to re-establish the initial tissue architecture and cardiac fibrosis settles.

7.1 - Future Perspectives

Albeit the herein MSc thesis incorporates novel insight about the neonatal cardiac injury, several experiments are still required to further understand the mechanisms and cellular/extracellular dynamics underlying apex resection in neonatal mice (Table 4).

Firstly, cardiac function evaluation 60 days post surgery would be a fundamental information, clarifying whether the scar expansion, from 21 to 60 days, could impact on heart function. Additionally, heart resistance to physical activity could be performed in 60 days-old injured mice to access the impact of fibrosis to support daily life activities. Concomitantly, it would be interesting to do an electrocardiographic analysis in order to confirm if the sub expression of Cx43 is affecting the normal impulse propagation and associated to cardiomyopathy.

Regarding cardiac fibroblast population, the dissection of different phenotypic profiles anticipates distinct performances on the cardiac injury response. In this sense, qPCR will be performed, envisioning the association of particular transcriptomic levels with populations with regenerative or reparative behavior.

Furthermore, to complete CM morphometric analysis, Langendorf–based isolation of adult CMs will further confirm the lack of hypertrophic parameters and the phenotype (rod or round) of adult CM. Unfortunately, this analysis was not possible during the development of the herein MSc thesis once the isolation protocol establish in our lab is not optimized for adult CMs.

Although CM proliferation was ascertained in the scope of this work, CM cytokinesis would be an important parameter to assess cardiomyocytic repopulation. In this sense, co localization of Aurora B kinase (AurB) with a CM marker would answer this purpose. In line with this, CM lineage tracing, through genetic fate mapping approach, would be a strategy to determine the origin of the new CM within the apex region.

A key question that arises from this work is whether CM proliferation is insufficient to fully restore the myocardium or if the regenerative mechanisms are halted by cardiac fibrosis. Drug administration for blocking TGF-β or inducible tissue-specific knockout for upstream targets of fibrosis would be possible approaches.

Furthermore, a deeper analysis of the ECM components might be important to design useful applications for clinical purposes such as biodegradable cardiac patches or engineer biomimetic matrices that promote regeneration rather than a scar-forming response. In this sense, primary cultures of CMs and/or cardiac fibroblasts onto different ECM-coated plates could give us new insights about proliferation and migration to optimize cardiac repair.

Table 4. Future perspectives - proposed aims and strategies.

Aim	Strategy
Assess cardiac function 60 days post-surgery	Echocardiography; electrocardiography and increase physical activity
Dissect the role of cardiac fibroblasts population	qPCR
Deeper analysis of neomyogenic potential	Imaging flow cytometry of Langerdorf isolated CMs and immunohistochemistry of AurB
Ascertain CM origin upon cardiac injury	CM lineage tracing
Assess the limiting mechanism (CM proliferation or fibrosis)	Inhibition of one of the process in vivo
Understand ECM-mediated cardiac cells behaviour *in vitro*	CM culture onto different ECM coated plates

Chapter 8

References

[1]   Mehra, R., *Global public health problem of sudden cardiac death.* J Electrocardiol, 2007. **40**(6 Suppl): p. S118-22.

[2]   Mathers, C.D. and D. Loncar, *Projections of Global Mortality and Burden of Disease from 2002 to 2030.* PLoS Med, 2006. **3**(11): p. e442.

[3]   Gaziano, T.A., *Cardiovascular disease in the developing world and its cost-effective management.* Circulation, 2005. **112**(23): p. 3547-53.

[4]   Nowbar, A.N., et al., *2014 Global geographic analysis of mortality from ischaemic heart disease by country, age and income: Statistics from World Health Organisation and United Nations.* International Journal of Cardiology, 2014. **174**(2): p. 293-298.

[5]   Smits, A. and P. Riley, *Epicardium-Derived Heart Repair.* Journal of Developmental Biology, 2014. **2**(2): p. 84-100.

[6]   Krenning, G., E.M. Zeisberg, and R. Kalluri, *The Origin of Fibroblasts and Mechanism of Cardiac Fibrosis.* Journal of cellular physiology, 2010. **225**(3): p. 631-637.

[7]   Kass, D.A., J.G.F. Bronzwaer, and W.J. Paulus, *What Mechanisms Underlie Diastolic Dysfunction in Heart Failure?* Circ Res, 2004. **94**(12): p. 1533-1542.

[8]   Stocum, D.L., *1 - An Overview of Regenerative Biology and Medicine*, in *Regenerative Biology and Medicine*, D.L. Stocum, Editor. 2006, Academic Press: Burlington. p. 1-20.

[9]   Carvalho, A.B. and A.C.C. de Carvalho, *Heart regeneration: Past, present and future.* World Journal of Cardiology, 2010. **2**(5): p. 107-111.

[10]   Beltrami, A.P., et al., *Evidence That Human Cardiac Myocytes Divide after Myocardial Infarction.* New England Journal of Medicine, 2001. **344**(23): p. 1750-1757.

[11]   Bergmann, O., et al., *Evidence for cardiomyocyte renewal in humans.* Science, 2009. **324**(5923): p. 98-102.

[12]   Laflamme, M.A. and C.E. Murry, *Heart regeneration.* Nature, 2011. **473**(7347): p. 326-35.

[13]   Xin, M., E.N. Olson, and R. Bassel-Duby, *Mending broken hearts: cardiac development as a basis for adult heart regeneration and repair.* Nat Rev Mol Cell Biol, 2013. **14**(8): p. 529-41.

[14]   Mollova, M., et al., *Cardiomyocyte proliferation contributes to heart growth in young humans.* Proceedings of the National Academy of Sciences of the United States of America, 2013. **110**(4): p. 1446-1451.

[15]   Beltrami, A.P., et al., *Adult Cardiac Stem Cells Are Multipotent and Support Myocardial Regeneration.* Cell, 2003. **114**(6): p. 763-776.

[16]   Oh, H., et al., *Cardiac progenitor cells from adult myocardium: Homing, differentiation, and fusion after infarction.* Proceedings of the National Academy of Sciences, 2003. **100**(21): p. 12313-12318.

[17]   Laugwitz, K.-L., et al., *Postnatal isl1+ cardioblasts enter fully differentiated cardiomyocyte lineages.* Nature, 2005. **433**(7026): p. 647-653.

[18]   Chong, J.J.H., et al., *Adult Cardiac-Resident MSC-like Stem Cells with a Proepicardial Origin.* Cell stem cell, 2011. **9**(6): p. 527-540.

[19]   Hudson, J. and E. Porrello, *The Non-coding Road Towards Cardiac Regeneration.* Journal of Cardiovascular Translational Research, 2013. **6**(6): p. 909-923.

[20]   Valente, M., et al., *Sca-1+ cardiac progenitor cells and heart-making: a critical synopsis.* Stem Cells Dev, 2014. **23**(19): p. 2263-73.

[21]   Bonauer, A., et al., *MicroRNA-92a controls angiogenesis and functional recovery of ischemic tissues in mice.* Science, 2009. **324**(5935): p. 1710-3.

[22]   Limana, F., et al., *HMGB1 attenuates cardiac remodelling in the failing heart via enhanced cardiac regeneration and miR-206-mediated inhibition of TIMP-3.* PLoS One, 2011. **6**(6): p. 22.

[23]   Ellison, G.M., et al., *Endogenous Cardiac Stem Cell Activation by Insulin-Like Growth Factor-1/Hepatocyte Growth Factor Intracoronary Injection Fosters Survival and Regeneration of the Infarcted Pig Heart.* Journal of the American College of Cardiology, 2011. **58**(9): p. 977-986.

[24]   Kanashiro-Takeuchi, R.M., et al., *Activation of growth hormone releasing hormone (GHRH) receptor stimulates cardiac reverse remodeling after myocardial infarction (MI).* Proceedings of the National Academy of Sciences, 2012. **109**(2): p. 559-563.

[25]   Bolli, R., et al., *Cardiac stem cells in patients with ischaemic cardiomyopathy (SCIPIO): initial results of a randomised phase 1 trial.* The Lancet. **378**(9806): p. 1847-1857.

[26]   Ishigami, S., et al., *Intracoronary Autologous Cardiac Progenitor Cell Transfer in Patients With Hypoplastic Left Heart Syndrome: The TICAP Prospective Phase 1 Controlled Trial.* Circulation Research, 2015. **116**(4): p. 653-664.

[27]   Nascimento, D., et al., *Human umbilical cord tissue-derived mesenchymal stromal cells attenuate remodeling after myocardial infarction by proangiogenic, antiapoptotic, and endogenous cell-activation mechanisms.* Stem Cell Research & Therapy, 2014. **5**(1): p. 5.

[28]   Wu, S.M., K.R. Chien, and C. Mummery, *Origins and Fates of Cardiovascular Progenitor Cells.* Cell, 2008. **132**(4): p. 537-543.

[29]   Kikuchi, K. and K.D. Poss, *Cardiac regenerative capacity and mechanisms.* Annu Rev Cell Dev Biol, 2012. **28**: p. 719-41.

[30]   Seifert, A. and S. Voss, *Revisiting the relationship between regenerative ability and aging.* BMC Biology, 2013. **11**(1): p. 2.

[31]   Drenckhahn, J.D., et al., *Compensatory growth of healthy cardiac cells in the presence of diseased cells restores tissue homeostasis during heart development.* Dev Cell, 2008. **15**(4): p. 521-33.

[32]   Porrello, E.R., et al., *Transient regenerative potential of the neonatal mouse heart.* Science, 2011. **331**(6020): p. 1078-80.

[33]   Haubner, B.J., et al., *Complete cardiac regeneration in a mouse model of myocardial infarction.* Aging (Albany NY), 2012. **4**(12): p. 966-77.

[34]   Jesty, S.A., et al., *c-kit+ precursors support postinfarction myogenesis in the neonatal, but not adult, heart.* Proc Natl Acad Sci U S A, 2012. **109**(33): p. 13380-5.

[35]   Porrello, E.R., et al., *Regulation of neonatal and adult mammalian heart regeneration by the miR-15 family.* Proc Natl Acad Sci U S A, 2013. **110**(1): p. 187-92.

[36]   Darehzereshki, A., et al., *Differential regenerative capacity of neonatal mouse hearts after cryoinjury.* Dev Biol, 2014.

[37]   Darehzereshki, A., et al., *Differential regenerative capacity of neonatal mouse hearts after cryoinjury.* Dev Biol, 2015. **399**(1): p. 91-9.

[38]   Konfino, T., et al., *The Type of Injury Dictates the Mode of Repair in Neonatal and Adult Heart.* Journal of the American Heart Association, 2015. **4**(1).

[39]   Kotlikoff, Michael I., M. Hesse, and Bernd K. Fleischmann, *Comment on "Do Neonatal Mouse Hearts Regenerate following Heart Apex Resection"?* Stem Cell Reports, 2014. **3**(1): p. 2.

[40]   Andersen, D.C., et al., *Do neonatal mouse hearts regenerate following heart apex resection?* Stem Cell Reports, 2014. **2**(4): p. 406-13.

[41]   Bryant, D.M., et al., *A systematic analysis of neonatal mouse heart regeneration after apical resection.* J Mol Cell Cardiol, 2015. **79**: p. 315-8.

[42]   Kotlikoff, M.I., M. Hesse, and B.K. Fleischmann, *Comment on "Do neonatal mouse hearts regenerate following heart apex resection"?* Stem Cell Reports, 2014. **3**(1): p. 2.

[43]   Alvarado, A.S. and P.A. Tsonis, *Bridging the regeneration gap: genetic insights from diverse animal models.* Nat Rev Genet, 2006. **7**(11): p. 873-884.

[44]   Bishopric, N.H., *Evolution of the Heart from Bacteria to Man.* Annals of the New York Academy of Sciences, 2005. **1047**(1): p. 13-29.

[45]   Oberpriller Jo Fau - Oberpriller, J.C. and J.C. Oberpriller, *Response of the adult newt ventricle to injury.* J Exp Zool, 1974. **187**(2): p. 249-53.

[46]   Poss, K.D., M.T. Wilson Lg Fau - Keating, and M.T. Keating, *Heart regeneration in zebrafish.* Science, 2002. **298**(5601): p. 2188-90.

[47]   Ausoni, S. and S. Sartore, *From fish to amphibians to mammals: in search of novel strategies to optimize cardiac regeneration.* The Journal of Cell Biology, 2009. **184**(3): p. 357-364.

[48]   Li, F., et al., *Rapid transition of cardiac myocytes from hyperplasia to hypertrophy during postnatal development.* J Mol Cell Cardiol, 1996. **28**(8): p. 1737-46.

[49]   Laflamme, M.A. and C.E. Murry, *Heart regeneration.* Nature. **473**(7347): p. 326-35.

[50]   Perez-Pomares, J.M., J.M. Gonzalez-Rosa, and R. Munoz-Chapuli, *Building the vertebrate heart - an evolutionary approach to cardiac development.* Int J Dev Biol, 2009. **53**(8-10): p. 1427-43.

[51]   Li, F., et al., *Rapid transition of cardiac myocytes from hyperplasia to hypertrophy during postnatal development.* J Mol Cell Cardiol, 1996. **28**(8): p. 1737-46.

[52]   Olivetti, G., et al., *Aging, Cardiac Hypertrophy and Ischemic Cardiomyopathy Do Not Affect the Proportion of Mononucleated and Multinucleated Myocytes in the Human Heart.* Journal of Molecular and Cellular Cardiology, 1996. **28**(7): p. 1463-1477.

[53]   Puente, B.N., et al., *The oxygen-rich postnatal environment induces cardiomyocyte cell-cycle arrest through DNA damage response.* Cell, 2014. **157**(3): p. 565-79.

[54]   Sander, V., et al., *Isolation and in vitro culture of primary cardiomyocytes from adult zebrafish hearts.* Nat Protoc, 2013. **8**(4): p. 800-9.

[55]   Paradis, A.N., M.S. Gay, and L. Zhang, *Binucleation of cardiomyocytes: the transition from a proliferative to a terminally differentiated state.* Drug Discov Today, 2014. **19**(5): p. 602-9.

[56]   Breckenridge, R., *Molecular Control of Cardiac Fetal/Neonatal Remodeling.* Journal of Cardiovascular Development and Disease, 2014. **1**(1): p. 29-36.

[57]   Pasumarthi, K.B.S. and L.J. Field, *Cardiomyocyte Cell Cycle Regulation.* Circulation Research, 2002. **90**(10): p. 1044-1054.

[58]   Muralidhar, S.A., et al., *Harnessing the power of dividing cardiomyocytes.* Glob Cardiol Sci Pract, 2013. **2013**(3): p. 212-21.

[59]   Adler, C.P. and U. Costabel, *Cell number in human heart in atrophy, hypertrophy, and under the influence of cytostatics.* Recent Adv Stud Cardiac Struct Metab, 1975. **6**: p. 343-55.

[60]   Pasumarthi, K.B., et al., *Targeted expression of cyclin D2 results in cardiomyocyte DNA synthesis and infarct regression in transgenic mice.* Circ Res, 2005. **96**(1): p. 110-8.

[61]   Li, J.M., G. Poolman Ra Fau - Brooks, and G. Brooks, *Role of G1 phase cyclins and cyclin-dependent kinases during cardiomyocyte hypertrophic growth in rats.* Am J Physiol, 1998. **275**(3 Pt 2): p. H814-22.

[62]   Flink, I.L., et al., *Changes in E2F complexes containing retinoblastoma protein family members and increased cyclin-dependent kinase inhibitor activities during terminal differentiation of cardiomyocytes.* J Mol Cell Cardiol, 1998. **30**(3): p. 563-78.

[63]   Sim, C.B., et al., *Dynamic changes in the cardiac methylome during postnatal development.* FASEB J, 2015. **29**(4): p. 1329-43.

[64]   Gilsbach, R., et al., *Dynamic DNA methylation orchestrates cardiomyocyte development, maturation and disease.* Nat Commun, 2014. **5**: p. 5288.

[65]   Sim, C.B., et al., *Dynamic changes in the cardiac methylome during postnatal development.* Faseb j, 2014.

[66]   Wadugu, B. and B. Kuhn, *The role of neuregulin/ErbB2/ErbB4 signaling in the heart with special focus on effects on cardiomyocyte proliferation.* Am J Physiol, 2012. **302**(11): p. H2139-47.

[67]   D'Uva, G., et al., *ERBB2 triggers mammalian heart regeneration by promoting cardiomyocyte dedifferentiation and proliferation.* Nature Cell Biology, 2015. **17**: p. 627-38.

[68]   Kubin, T., et al., *Oncostatin M is a major mediator of cardiomyocyte dedifferentiation and remodeling.* Cell Stem Cell, 2011. **9**(5): p. 420-32.

[69]   Bersell, K., et al., *Neuregulin1/ErbB4 signaling induces cardiomyocyte proliferation and repair of heart injury.* Cell, 2009. **138**(2): p. 257-70.

[70]   Xin, M., et al., *Regulation of insulin-like growth factor signaling by Yap governs cardiomyocyte proliferation and embryonic heart size.* Sci Signal, 2011. **4**(196): p. ra70.

[71]   Heallen, T., et al., *Hippo signaling impedes adult heart regeneration.* Development, 2013. **140**(23): p. 4683-90.

[72]   von Gise, A., et al., *YAP1, the nuclear target of Hippo signaling, stimulates heart growth through cardiomyocyte proliferation but not hypertrophy.* PNAS, 2011. **109**(7): p. 2394-99.

[73]   Senyo, S.E., R.T. Lee, and B. Kühn, *Cardiac regeneration based on mechanisms of cardiomyocyte proliferation and differentiation.* Stem Cell Research, 2014. **13**(3, Part B): p. 532-541.

[74]   Parker, T.G., M.D. Packer Se Fau - Schneider, and M.D. Schneider, *Peptide growth factors can provoke "fetal" contractile protein gene expression in rat cardiac myocytes.* J Clin Invest, 1990. **85**(2): p. 507-14.

[75]   Engel, F.B., et al., *p38 MAP kinase inhibition enables proliferation of adult mammalian cardiomyocytes.* Genes & Development, 2005. **19**(10): p. 1175-1187.

[76]   Kuhn, B., et al., *Periostin induces proliferation of differentiated cardiomyocytes and promotes cardiac repair.* Nat Med, 2007. **13**(8): p. 962-969.

[77]   Eulalio, A., et al., *Functional screening identifies miRNAs inducing cardiac regeneration.* Nature, 2012. **492**(7429): p. 376-381.

[78]   Pandey, R. and R.P. Ahmed, *MicroRNAs Inducing Proliferation of Quiescent Adult Cardiomyocytes.* Cardiovascular Regenerative Medicine, 2015. **2**(1).

[79]   Miyamoto, S., et al., *Integrin function: molecular hierarchies of cytoskeletal and signaling molecules.* J Cell Biol, 1995. **131**(3): p. 791-805.

[80]   Bashey, R.I., et al., *Growth properties and biochemical characterization of collagens synthesized by adult rat heart fibroblasts in culture.* J Mol Cell Cardiol, 1992. **24**(7): p. 691-700.

[81]   Bayomy, A.F., et al., *Regeneration in heart disease-Is ECM the key?* Life Sci, 1992. **91**(17-18): p. 823-7.

[82]   Burgess, M.L., H.L. McCrea Jc Fau - Hedrick, and H.L. Hedrick, *Age-associated changes in cardiac matrix and integrins.* Mech Ageing Dev, 2001. **122**(15): p. 1739-56.

[83]   Faucherre, A. and C. Jopling, *The heart's content-renewable resources.* International Journal of Cardiology, 2013. **167**(4): p. 1141-1146.

[84]   Schulz, R., et al., *Connexin 43 is an emerging therapeutic target in ischemia/reperfusion injury, cardioprotection and neuroprotection.* Pharmacology & Therapeutics, 2015. **153**: p. 90-106.

[85]   Zogbi, C., et al., *Early postnatal rat ventricle resection leads to long-term preserved cardiac function despite tissue hypoperfusion.* Physiological Reports, 2014. **2**(8): p. e12115.

[86]   Seidel, T., A. Salameh, and S. Dhein, *A Simulation Study of Cellular Hypertrophy and Connexin Lateralization in Cardiac Tissue.* Biophysical Journal, 2010. **99**(9): p. 2821-2830.

[87]   Strungs, E.G., et al., *Cryoinjury models of the adult and neonatal mouse heart for studies of scarring and regeneration.* Methods in Molecular Biology, 2013. **1037**: p. 343-53.

[88]   Ausma, J., et al., *Dedifferentiated cardiomyocytes from chronic hibernating myocardium are ischemia-tolerant.* Mol Cell Biochem, 1998. **186**(1-2): p. 159-68.

[89]   Wijns, W., P.G. Vatner Sf Fau - Camici, and P.G. Camici, *Hibernating myocardium.* N Engl J Med, 1998. **339**(3): p. 173-81.

[90]   Frangogiannis, N.G., *The inflammatory response in myocardial injury, repair, and remodelling.* Nat Rev Cardiol, 2014. **11**(5): p. 255-265.

[91]   Haynes, B.F., et al., *Early events in human T cell ontogeny. Phenotypic characterization and immunohistologic localization of T cell precursors in early human fetal tissues.* The Journal of Experimental Medicine, 1988. **168**(3): p. 1061-1080.

[92]   Trowsdale, J. and A.G. Betz, *Mother's little helpers: mechanisms of maternal-fetal tolerance.* Nat Immunol, 2006. **7**(3): p. 241-246.

[93]   Kyritsis, N., et al., *Acute Inflammation Initiates the Regenerative Response in the Adult Zebrafish Brain.* Science, 2012. **338**(6112): p. 1353-1356.

[94]   Godwin, J.W. and J.P. Brockes, *Regeneration, tissue injury and the immune response.* Journal of Anantomy, 2006. **209**(4): p. 423-32.

[95]   Mescher, A.L. and A.W. Neff, *Limb regeneration in amphibians: immunological considerations.* Scientific World Journal Suppl 2006. **Suppl 1**(6): p. 1-11.

[96]   Godwin, J.W. and N. Rosenthal, *Scar-free wound healing and regeneration in amphibians: Immunological influences on regenerative success.* Differentiation, 2014. **87**(1-2): p. 66-75.

[97]   Aurora, A.B., et al., *Macrophages are required for neonatal heart regeneration.* The Journal of Clinical Investigation, 2014. **124**(3): p. 1382-1392.

[98]   Lavine, K.J., et al., *Distinct macrophage lineages contribute to disparate patterns of cardiac recovery and remodeling in the neonatal and adult heart.* Proc Natl Acad Sci U S A, 2014. **111**(45): p. 16029-34.

[99]   Wang, J., et al., *Fibronectin is deposited by injury-activated epicardial cells and is necessary for zebrafish heart regeneration.* Dev Biol, 2013. **382**(2): p. 427-35.

[100]   Mercer, S.E., H.-G. Odelberg Sj Fau - Simon, and H.G. Simon, *A dynamic spatiotemporal extracellular matrix facilitates epicardial-mediated vertebrate heart regeneration.* Dev Biol, 2013. **382**(2): p. 457-69.

[101]   Rybarczyk, B.J., P.J. Lawrence So Fau - Simpson-Haidaris, and P.J. Simpson-Haidaris, *Matrix-fibrinogen enhances wound closure by increasing both cell proliferation and migration.* Blood, 2003. **102**(12): p. 4035-43.

[102]   Sivakumar, P., et al., *Upregulation of lysyl oxidase and MMPs during cardiac remodeling in human dilated cardiomyopathy.* Mol Cell Biochem, 2008. **307**(1): p. 159-67.

[103]   Baudino, T.A., et al., *Cardiac fibroblasts: friend or foe?* Am J Physiol 2006. **291**(3): p. 1015-26.

[104]   Ieda, M., et al., *Cardiac Fibroblasts Regulate Myocardial Proliferation through β1 Integrin Signaling.* Developmental cell, 2009. **16**(2): p. 233-244.

[105]   Mahmoud, A.I. and E.R. Porrello, *Turning back the cardiac regenerative clock: lessons from the neonate.* Trends Cardivasc Med, 2012. **22**(5): p. 128-33.

[106] Banerjee, I., et al., *Determination of cell types and numbers during cardiac development in the neonatal and adult rat and mouse.* 2007(0363-6135 (Print)).

[107] Norris, R.A., et al., *Neonatal and adult cardiovascular pathophysiological remodeling and repair: developmental role of periostin.* Ann NY Acad Sci, 2008. **1123**: p. 30-40.

[108] Miragoli, M., S. Gaudesius G Fau - Rohr, and S. Rohr, *Electrotonic modulation of cardiac impulse conduction by myofibroblasts.* 2006(1524-4571 (Electronic)).

[109] Dobaczewski, M., N.G. de Haan Jj Fau - Frangogiannis, and N.G. Frangogiannis, *The extracellular matrix modulates fibroblast phenotype and function in the infarcted myocardium.* 2012(1937-5395 (Electronic)).

[110] Mann, D.L., *The emerging role of innate immunity in the heart and vascular system: for whom the cell tolls.* Circulation research, 2011. **108**(9): p. 1133-1145.

[111] Frangogiannis, N.G., M.L. Michael Lh Fau - Entman, and M.L. Entman, *Myofibroblasts in reperfused myocardial infarcts express the embryonic form of smooth muscle myosin heavy chain (SMemb).* Cardiovasc Res, 2000. **48**(1): p. 89-100.

[112] Willems, I.E., et al., *The alpha-smooth muscle actin-positive cells in healing human myocardial scars.* Am J Physiol, 1994. **145**(4): p. 868-75.

[113] Yang, F., et al., *Myocardial infarction and cardiac remodelling in mice.* Exp Physiol, 2002. **87**(5): p. 547-55.

[114] Speiser, B., et al., *The extracellular matrix in human cardiac tissue. Part II: Vimentin, laminin, and fibronectin.* Cardioscience, 1992. **3**(1): p. 41-9.

[115] Osterreicher, C.H., et al., *Fibroblast-specific protein 1 identifies an inflammatory subpopulation of macrophages in the liver.* Proc Natl Acad Sci USA, 2011. **108**(1): p. 308-13.

[116] Madi, H.A., et al., *Inherent differences in morphology, proliferation, and migration in saphenous vein smooth muscle cells cultured from nondiabetic and Type 2 diabetic patients.* Am J Physiol, 2009. **297**(5): p. C1307-17.

[117] Hudon-David, F., et al., *Thy-1 expression by cardiac fibroblasts: lack of association with myofibroblast contractile markers.* J Mol Cell Cardiol, 2007. **42**(5): p. 991-1000.

[118] Acharya, A., et al., *The bHLH transcription factor Tcf21 is required for lineage-specific EMT of cardiac fibroblast progenitors.* Development, 2012. **139**(12): p. 2139-49.

[119] Goldsmith, E.C., et al., *Organization of fibroblasts in the heart.* Dev Dyn, 2004. **230**(4): p. 787-94.

[120] Kern, C.B., et al., *Immunolocalization of chick periostin protein in the developing heart.* Anat Rec A Discov Mol Cell Evol Biol, 2005. **284**(1): p. 415-23.

[121] Wang, X., et al., *The Role of the Sca-1+/CD31– Cardiac Progenitor Cell Population in Postinfarction Left Ventricular Remodeling.* STEM CELLS, 2006. **24**(7): p. 1779-1788.

[122] Smith, C.L., et al., *Epicardial derived cell epithelial to mesenchymal transition and fate specification require PDGF receptor signaling.* Circulation research, 2011. **108**(12): p. e15-e26.

[123] Midgley, A.C., et al., *Transforming growth factor-beta1 (TGF-beta1)-stimulated fibroblast to myofibroblast differentiation is mediated by hyaluronan (HA)-facilitated epidermal growth factor receptor (EGFR) and CD44 co-localization in lipid rafts.* J Biol Chem, 2013. **288**(21): p. 14824-38.

[124] Clark, R.A., et al., *Fibroblast invasive migration into fibronectin/fibrin gels requires a previously uncharacterized dermatan sulfate-CD44 proteoglycan.* J Invest Dermatol, 2004. **122**(2): p. 266-77.

[125] Lu, Q.L. and T.A. Partridge, *A new blocking method for application of murine monoclonal antibody to mouse tissue sections.* J Histochem Cytochem, 1998. **46**(8): p. 977-84.

[126] Collesi, C., et al., *Notch1 signaling stimulates proliferation of immature cardiomyocytes.* The Journal of Cell Biology, 2008. **183**(1): p. 117-128.

[127] Greiling, D. and R.A. Clark, *Fibronectin provides a conduit for fibroblast transmigration from collagenous stroma into fibrin clot provisional matrix.* J Cell Sci, 1997. **110**(7): p. 861-70.

[128] Leask, A., *TGFbeta, cardiac fibroblasts, and the fibrotic response.* Cardiovasc Res, 2007. **74**(2): p. 207-12.

[129] Savic-Radojevic, A., et al., *The role of serum VCAM-1 and TNF-alpha as predictors of mortality and morbidity in patients with chronic heart failure*. J Clin Lab Anal, 2013. **27**(2): p. 105-12.

[130] Keon, W.J., *Heart transplantation in perspective*. J Card Surg, 1999. **14**(2): p. 147-51.

[131] Heber-Katz, E., *The regenerating mouse ear*. Semin Cell Dev Biol, 1999. **10**(4): p. 415-9.

[132] Porrello, E.R. and E.N. Olson, *A neonatal blueprint for cardiac regeneration*. Stem Cell Research, 2014. **13**(3, Part B): p. 556-570.

[133] Szibor, M., et al., *Remodeling and dedifferentiation of adult cardiomyocytes during disease and regeneration*. Cellular and Molecular Life Sciences, 2014. **71**(10): p. 1907-1916.

[134] Peters, N.S., *Myocardial gap junction organization in ischemia and infarction*. Micros Res Tech, 1995. **31**(5): p. 375-86.

[135] Danon, A., et al., *Hypoxia causes connexin 43 internalization in neonatal rat ventricular myocytes*. Gen Physiol Biophys, 2010. **29**(3): p. 222-33.

[136] Jansen, J.A., et al., *Reduced Cx43 Expression Triggers Increased Fibrosis Due to Enhanced Fibroblast Activity*. Circulation: Arrhythmia and Electrophysiology, 2012. **5**(2): p. 380-390.

[137] Stoffels, J.M., W. Zhao C Fau - Baron, and W. Baron, *Fibronectin in tissue regeneration: timely disassembly of the scaffold is necessary to complete the build*. Cell Mol Life Sci, 2013. **70**(22): p. 4243-53.

[138] Imanaka-Yoshida, K., T. Hiroe M Fau - Yoshida, and T. Yoshida, *Interaction between cell and extracellular matrix in heart disease: multiple roles of tenascin-C in tissue remodeling*. Histol Histopathol, 2004. **19**(2): p. 517-25.

[139] Chablais, F., et al., *The zebrafish heart regenerates after cryoinjury-induced myocardial infarction*. BMC Developmental Biology, 2011. **11**(1): p. 21.

[140] Willems, I.E.M.G., J.-W. Arends, and M.J.A.P. Daemen, *Tenascin and Fibronectin expression in healing human myocardial scars*. The Journal of Pathology, 1996. **179**(3): p. 321-325.

[141] Acharya, P.S., et al., *Fibroblast migration is mediated by CD44-dependent TGF beta activation*. J Cell Sci, 2000. **121**(Pt 9): p. 1393-402.

[142] Kapur, N.K., et al., *Reduced endoglin activity limits cardiac fibrosis and improves survival in heart failure*. Circulation, 2012. **125**(22): p. 2728-38.

[143] Sadek, H.A., et al., *Multi-investigator letter on reproducibility of neonatal heart regeneration following apical resection*. Stem Cell Reports, 2014. **3**(1): p. 1.

[144] Andersen, D.C., C.H. Jensen, and S.P. Sheikh, *Response to Sadek et al. and Kotlikoff et al*. Stem Cell Reports, 2014. **3**(1): p. 3-4.